Interhemispheric Comparisons of Structure and Variability of the Quasi-2-Day Wave at Middle and High Latitudes

Hiroyuki Iimura[1], David C. Fritts[2], Ruth S. Lieberman[3], Diego Janches[4], Nicholas John Mitchell[5], Werner Singer[6], Steven J. Franke[7], and Wayne K. Hocking[8]

[1]GATS Inc.
[2]GATS
[3]NASA Goddard
[4]National Aeronautics and Space Administration (NASA)
[5]University of Bath
[6]Leibniz-Institute of Atmospheric Physics (LG)
[7]University of Illinois at Urbana Champaign
[8]University of Western Ontario

November 25, 2022

Abstract

Structure of the quasi-2-day wave (Q2DW) in the mesosphere and lower thermosphere (MLT) was compared between the northern and southern hemispheres, employing temperature and geopotential height data obtained from the Microwave Limb Sounder (MLS) onboard NASA's Earth Observing System (EOS) Aura satellite. The Q2DW in horizontal winds was derived using balance equations with MLS geopotential height data. Amplitudes were maximized at ˜40° in summer with larger amplitudes in the meridional wind than the zonal wind in both hemispheres, but with much larger amplitudes in the southern hemisphere and a longer duration of enhancements in the northern hemisphere. Weaker enhancements were exhibited in winter in both hemispheres, but maximized at higher latitudes only in the southern hemisphere meridional component. Responses were moderately enhanced from late April to early May only in the southern hemisphere. The westward propagating zonal wavenumber 3 (W3) was largest in summer in both hemispheres, but the Q2DW comprised superposition with other modes in winter. Eliassen-Palm fluxes were derived for each mode. In the southern hemisphere, W3, W2, and W1 in January exhibited upward fluxes at lower latitudes, poleward fluxes at lower altitudes and equatorward fluxes at higher altitudes. A W3 mode in July in the northern hemisphere, on the other hand, exhibited upward and poleward fluxes in the entire altitude range. The Q2DW balance winds were compared with the radar winds. They agreed reasonably in amplitude and phase in summer in the southern hemisphere and lower latitudes in summer in the northern hemisphere and in winter hemispheres.

Interhemispheric Comparisons of Structure and Variability of the Quasi-2-Day Wave at Middle and High Latitudes

Hiroyuki Iimura[1], David C. Fritts[1], Ruth S. Lieberman[2], Diego Janches[2], Nicholas J. Mitchell[3], Steven J. Franke[4], Werner Singer[5], and Wayne K. Hocking[6]

[1]GATS Inc., Boulder, CO

[2]NASA Goddard Space Flight Center, Greenbelt, MD

[3]Department of Electronic and Electrical Engineering, University of Bath, Bath, UK

[4]Department of Electrical and Computer Engineering, University, UIUC, IL

[5]Leibniz Institute of Atmospheric Physics, Rostock University, Kühlungsborn, Germany

[6]Department of Physics, University of Western Ontario, London, Ontario, Canada

Corresponding author: Hiroyuki Iimura

Email: iimura@gats-inc.com

Phone: 720-274-4747

Key words: mesosphere and lower thermosphere, quasi-2-day wave, planetary wave, Eliassen-Palm fluxes, Aura/MLS, meteor radar

Index terms: 3332, 3334, 3346

Key points:

- The Q2DW at middle and high latitudes in January and July 2012 were compared between the northern and southern hemispheres.
- The Q2DW in horizontal wind fields were derived employing balance winds with Aura/MLS geopotential height data.
- Amplitudes in summer were larger in the southern hemisphere than the northern hemisphere due to large enhancements of W3.

Submitted to JGR Atmospheres 6 January 2020

Abstract

Structure of the quasi-2-day wave (Q2DW) in the mesosphere and lower thermosphere (MLT) was compared between the northern and southern hemispheres, employing temperature and geopotential height data obtained from the Microwave Limb Sounder (MLS) onboard NASA's Earth Observing System (EOS) Aura satellite. The Q2DW in horizontal winds was derived using balance equations with MLS geopotential height data. Amplitudes were maximized at ~40° in summer with larger amplitudes in the meridional wind than the zonal wind in both hemispheres, but with much larger amplitudes in the southern hemisphere and a longer duration of enhancements in the northern hemisphere. Weaker enhancements were exhibited in winter in both hemispheres, but maximized at higher latitudes only in the southern hemisphere meridional component. Responses were moderately enhanced from late April to early May only in the southern hemisphere. The westward propagating zonal wavenumber 3 (W3) was largest in summer in both hemispheres, but the Q2DW comprised superposition with other modes in winter. Eliassen-Palm fluxes were derived for each mode. In the southern hemisphere, W3, W2, and W1 in January exhibited upward fluxes at lower latitudes, poleward fluxes at lower altitudes and equatorward fluxes at higher altitudes. A W3 mode in July in the northern hemisphere, on the other hand, exhibited upward and poleward fluxes in the entire altitude range. The Q2DW balance winds were compared with the radar winds. They agreed reasonably in amplitude and phase in summer in the southern hemisphere and lower latitudes in summer in the northern hemisphere and in winter hemispheres.

1. Introduction

The quasi-2-day wave (Q2DW) is a global phenomenon and, since its discovery, has been observed in atmosphere from earth's surface through the troposphere to the thermosphere. In particular, the Q2DW in the mesosphere and lower thermosphere (MLT) has been observed by ground-based and satellite measurements (Bristow et al., 1999; Fritts et al., 1999; Kulikov, 2007; Li et al., 2008; Morris et al., 2009; Riggin et al., 2004; Sandford et al., 2008).

Salby (1980, 1981a, 1981b) proposed that the Q2DW is a manifestation of the mixed Rossby-gravity (3, 0) normal mode with a period of ~2.25 days and Pfister (1985) inferred wave growth of zonal wavenumbers 2, 3, and 4 with periods of ~2 days. Hagan et al. (1993) inferred that the (3, 0) mode is sensitive to zonal mean winds, especially a combination of weak eastward winds in the northern hemisphere and westward winds in the MLT in the southern hemisphere. Plumb (1983) theoretically predicted a growth of the Q2DW by baroclinic instabilities caused by an eastward shear in a westward jet, and this was investigated employing satellite observations (Gu et al., 2013; Lieberman, 1999; Limpasuvan and Dong, 2009).

Assessments of relations between the Q2DW and baroclinic/barotropic instabilities have also been examined employing model simulations (Baumgaertner et al., 2008; Guharay et al., 2013; McCormack et al., 2009; Merzlyakov and Jacobi, 2004; Rojas and Norton, 2007; Salby and Callagham, 2001, 2003; Schröder and Schmitz, 2004; Yue et al., 2012b) although Hunt (1981) showed only minimal baroclinic activity. Furthermore, Jia et al. (2012) and Offermann et al. (2011) inferred that Q2DW amplitudes correspond to the meridional gradient of the quasi-geostrophic potential vorticity; and Salby (1981c) concluded that Q2DW amplitudes grow with altitude where refractive index increases and temperature decreases equatorward. Pendlebury (2012) suggested a significant source of Q2DW variability for polar mesospheric clouds, Gurubaran et al. (2001a) found a correlation with the equatorial electrojet, and Sonnemann and Grygalashvyly (2005) found a 2-day oscillation in a photochemical system in the MLT.

Q2DW analyses employing ground-based radar wind measurements at various locations have shown that Q2DW responses are enhanced in summer and winter with meridional amplitudes larger than zonal amplitudes. Although the response is maximized in late January in the southern hemisphere (Hecht, 2010; Lima et al., 2012; Murphy and Vincent, 1998; Poole, 1990; Poole and Harris, 1995; Takahashi et al., 2012), amplitudes in the northern hemisphere are larger primarily in summer (Chshyolkova et al., 2005; Jacobi et al., 1997, 1998; Malinga and Ruohoniemi, 2007; Namboothiri et al., 2002; Thayaparan et al., 1997a, 1997b), but can also be larger in winter (Gurubaran et al., 2001b; Nozawa et al., 2003a). A vertical wavelength is variable at 25 – 100 km at low and equatorial latitudes (Araújo et al., 2014; Gurubaran et al., 2001b; Harris et al., 2013; Lima et al., 2004) but >150 km at middle latitudes (Craig and Elford, 1981; Harris, 1994; Tsuda et al., 1988).

Interhemispheric comparisons of simultaneous radar wind measurements at middle latitudes (Craig et al., 1983; Tsuda et al., 1988) and high latitudes (Tunbridge and Mitchell, 2009) revealed that Q2DW amplitudes in summer were larger in the southern hemisphere than northern hemisphere for both zonal and meridional components.

By combining radar wind measurements at multiple locations, discrepancies from westward propagating zonal wavenumber (W3) structure were found in January in both southern (Craig et al., 1980) and northern (Nozawa et al., 2003b) hemispheres. At middle latitudes in the northern hemisphere, Meek et al. (1996) found W3 as well as westward propagating zonal wavenumber 4 (W4), Merzlyakov et al. (2004) found westward propagating zonal wavenumber 2 (W2), W3, and W4 in 80, 60, and 48 hours, respectively, and Pancheva et al. (2004) found W2, W3, and W4 in 53-56, 48-50, and 42-43 hours, respectively. At low latitudes in the northern hemisphere, Pancheva et al. (2006) and Kumar et al. (2018) found W2 in the Q2DW.

The spatial structure of Q2DW zonal wavenumbers has been studied employing satellite measurements of winds (Ward et al., 1996; Wu et al., 1993), temperature (Huang et al., 2013; Rogers and Prata, 1981; Tunbridge et al., 2011; Wu et al., 1996), OH airglow (Pedatella and Forbes, 2012), water vapor (Limpasuvan and Leovy, 1995; Limpasuvan and Wu, 2003), and ozone density (Azeem et al., 2001). These satellites include Nimbus 5 Selective Chopper Radiometer (SCR), Nimbus 6 Pressure Modulated Radiometer (PMR), Microwave Limb Sounder (MLS) onboard Upper Atmosphere Research Satellite (UARS) and the Earth Observing System (EOS) Aura satellite, the High Resolution Doppler Imager (HRDI) and the Wind Imaging Interferometer (WINDII) onboard UARS, and the Sounding of the Atmosphere using Broadband Emission Radiometry (SABER) onboard the Thermosphere Ionosphere Mesosphere Energectics Dynamics (TIMED) satellite. Their results showed that

1. Q2DW amplitudes in summer enhancements were much larger in the southern hemisphere than the northern hemisphere,

2. the W3 mode was dominant during the summer enhancements in the southern hemisphere, maximizing at ~30°S while a mixture of the W3, W4, and W2 modes in the northern hemisphere, and

3. the Q2DW was anti-symmetric with respect to the equator.

Recently, Fritts et al. (2019) exhibited spatial structure of the Q2DW in horizontal winds in January 2015 southern hemisphere, deriving from balance equations with MLS geopotential height data. The wind data reasonably agreed with the Q2DW employing radar wind measurements. They also showed Eliassen-Palm (EP) fluxes for each Q2DW zonal wavenumber. We will apply their analyses to compare the Q2DW in the southern and northern hemisphere in January and July 2012. Because we slightly modified their methodology to estimate Q2DW winds inferred from MLS/balance equations, our methodology is explained in the next section. Results are presented in section 3. Discussion and summary are described in sections 4 and 5.

2. Data Acquisition and Analysis Methodology

2.1. Aura/MLS

The NASA's EOS Aura satellite launched on 25 July 2004 into a near-polar 705 km altitude sun-synchronous orbit. The satellite orbits ~15 times per day. The MLS onboard Aura began observing thermal microwave emission from Earth on 14 August 2004 at 55 pressure levels between 1,000 and 10^{-5} hPa. The MLS measures global atmospheric temperature and constituents day and night. Geopotential height is computed from integration of the hydrostatic equation (Schwarts et al., 2008).

We basically followed the analysis methodology of Fritts et al. (2019) for Q2DW zonal and meridional winds from MLS data. However, their methodology is valid only when the Q2DW dominates atmospheric waves, e.g., January in the southern hemisphere. To analyze seasonal variabilities of the Q2DW in both northern and southern hemispheres extracting from longer-period planetary waves, we modified their methodology slightly. Aura/MLS temperature and geopotential height data were collected in bins of 24° in longitude, 5° in latitude, and 12-hour universal time (UT) for each altitude between 75 and 118 km from 2010 to 2012. Then, 10-day zonal mean temperature and geopotential height were computed.

If the data were collected continuously, all bins were filled by data. However, data are missing from March to April 2011, and in February and March 2012 (see blank spaces in Figures 1 and 2). These bins were interpolated by a cubic spline with three degrees of freedom, and a band-pass filter from 42 and 54 hours was applied to time series for each longitude, latitude, and altitude. The band-pass filtered data enabled 10-day least-square fits to sinusoids with westward propagating zonal wavenumbers 1, 2, 3, and 4 (W1, W2, W3, and W4), zonally symmetric mode (S0), and eastward propagating zonal wavenumbers 1 and 2 (E1 and E2) for a 48-hour period.

Amplitudes and phases in zonal and meridional winds for each zonal wavenumber were estimated from geopotential height Q2DW amplitudes and phases employing zonal and meridional momentum equations (Hitchman et al., 1987),

$$\partial u'/\partial t + \bar{u}\,(\partial u'/\partial \lambda) / (a \cos\phi) - f_1 v' = -(\partial \Phi'/\partial \lambda) / (a \cos\phi), \qquad (1)$$

and

$$\partial v'/\partial t + \bar{u}\,(\partial v'/\partial \lambda) / (a \cos\phi) - f_2 u' = -(\partial \Phi'/\partial \phi) / a, \qquad (2)$$

where u', v', and Φ' are perturbations of zonal and meridional winds, and geopotential height, ϕ and λ are latitude and longitude, a is Earth's radius, and $\bar{u}$ is a zonal mean zonal wind, which were estimated from zonal mean geopotential heights, assuming gradient wind balance (Hitchman and Leovy, 1987; Hitchman et al., 1987),

$$\bar{u} = -(1/f)\,(\partial \Phi'/\partial y)\,[1 - (1/f)\,(\partial \Phi'/\partial y) / (2\Omega a \cos\phi)]^{-1}, \qquad (3)$$

where $\Omega = 2\pi$ (day^{-1}) and $f = 2\Omega \sin\phi$. f_1 and f_2 are defined as

$$f_1 = 2\Omega \sin\phi - [\partial(\bar{u} \cos\phi) / \partial\phi] / (a \cos\phi), \qquad (4)$$

and

$$f_2 = 2\Omega \sin\phi + 2\bar{u} \tan\phi / a. \qquad (5)$$

The meridional and altitudinal components of EP flux (Andrews et al., 1987) were computed by

$$F^{\phi} = (\partial \bar{u} / \partial z)\, \langle v'\theta' \rangle / (\partial \theta_0 / \partial z) - \langle u'v' \rangle, \qquad (6)$$

and

$$F^{z} = [f - (a \cos\phi)^{-1}\, \partial(\bar{u} \cos\phi) / \partial\phi]\, \langle v'\theta' \rangle / (\partial \theta_0 / \partial z) - \langle u'w' \rangle, \qquad (7)$$

where θ is geopotential temperature and <> indicates a zonal mean. EP fluxes presented in the next section were normalized by $\rho_0 a \cos\phi$ for both components.

2.2 Meteor Radars

Six meteor radars were employed at roughly conjugate latitudes in each hemisphere to compare with MLS/balance winds. All of these are All-Sky Interferometric Meteor Radar (SkiYMet) located at Esrange (68°N, 21°E), Juliusruh (55°N, 14°E), Bear Lake Observatory (42°N, 111°W), Cerro Pachón (30°S, 71°W), Tierra del Fuego (54°S, 68°W), and Rothera Station (68°S, 68°W) to minimize systematic biases and determine hourly winds under the same conditions. Determinations of hourly winds are described by Iimura et al. (2015). Meteor echo data at 90 ± 1.5 km were collected, which had radial velocities <150 km and zenith angles between 10 and 70°, and hourly mean zonal and meridional winds were computed if there were at least five echoes. Missing hourly points were interpolated by a cubic spline with three degrees of freedom and time series of the Q2DW were determined by inversed fast Fourier transform with a band-pass filter at 42 and 56 hours. Amplitudes and phases of the 10-day mean Q2DW were estimated by least-square fits to sinusoids with 48 hours.

3. Results

3.1. Spatial Structure

Figures 1 and 2 show seasonal variability of zonal and meridional Q2DW amplitudes at 6 latitudes from January 2011 to August 2012. In the northern hemisphere, amplitudes generally increased with altitude and equatorward with slightly larger amplitudes in the meridional component than the zonal component. Amplitudes reached ~20 ms^{-1} at 90 km in January and

July 2012. Amplitudes in the southern hemisphere generally increased with altitude and equatorward in both components and were enhanced in January and late April to May. Amplitudes maximized at ~66 ms^{-1} at 118 km and 40°S in January 2012 in the meridional component, zonal amplitudes reached at >45 ms^{-1} in January 2011 and 2012 and May 2011.

The upper panels of Figure 3 show latitudinal variability of Q2DW amplitudes at 91 km from July 2011 to August 2012. As shown in Figures 1 and 2, amplitudes increased equatorward in both components and hemispheres. In the northern hemisphere, amplitudes were enhanced in January and July with larger July amplitudes in 2012 than 2011. In the southern hemisphere, amplitude enhancement lasted during the entire month of January 2012 and from mid-April to early May 2012. During the latter enhancement, the maximum was larger in the zonal component, but the latitudinal range of the enhancement was wider in the meridional component.

Lower panels of Figure 3 compare latitudinal structure of Q2DW amplitudes in the northern and southern hemispheres in January and July at 91 km. In January, amplitudes maximized at lower latitudes in both hemispheres but earlier in the northern hemisphere than the southern hemisphere for both components. Amplitude enhancements lasted longer in the meridional component than the zonal component. In July, on the other hand, amplitude maximized at ~45°N in the zonal component while amplitude increased equatorward in the meridional component. In the southern hemisphere, amplitudes maximized at higher latitudes of ~60°S at the middle of the month in the meridional component while no clear enhancements were observed in the zonal component.

Figure 4 shows latitude variabilities of amplitudes for each Q2DW zonal wavenumber at 91 km in January 2012. All modes were larger in the southern hemisphere than the northern hemisphere and maximized at lower latitudes, except for S0. Meridional amplitudes were larger than zonal amplitudes for W4, W3, and W2 while zonal amplitudes were larger for W1, S0, E1, and E2. W4 and W2 maximized early in the month for both components. W3 and W1 weakened at mid-month, and hence, were enhanced before and after the weakening. S0 was enhanced at middle latitudes at mid-month and eastward modes were enhanced slightly later in the month. Amplitude enhancements at lower latitudes indicated cross-equatorial propagations in W4, W2, W3, and S0; however, cross-equatorial propagations were not clear for W1 and eastward modes.

Similarly, Figure 5 shows latitude variabilities of amplitudes in July 2012. Amplitudes were larger in the northern hemisphere for all modes; however, meridional amplitudes were larger only for W4 and W3. W4 maximized early in the month while W3 maximized at mid-month. Maxima of W2 amplitudes were similar for both components and coincided with W3. Maxima of zonal amplitudes were larger than the meridional maxima for W1, S0, and eastward modes. Both W1 and E1 maximized at lower latitudes but earlier for W1 than E1. E2 maximized at middle latitudes later in the month and S0 maximized at higher latitudes early in the month. Cross-equatorial propagations were inferred in W2, W1, and E1.

Figure 6 shows latitude/longitude structure of Q2DW wind and temperature for each zonal wavenumber and sum of all zonal wavenumbers at 91 km at 12:30 on 11 January 2012. Amplitudes were larger in the southern hemisphere than the northern hemisphere for all modes for both temperature and winds and generally increased equatorward for westward propagations in both hemispheres. Phase structure with respect to the equator was:

W4: symmetric (anti-symmetric) at lower latitudes and anti-symmetric (symmetric) at higher latitudes in temperature (zonal wind), and anti-symmetric at higher latitudes in meridional wind,

W3: anti-symmetric in temperature and zonal wind, and symmetric (anti-symmetric) at lower (higher) latitudes in meridional wind,

W2: anti-symmetric (symmetric) in temperature (zonal wind), and symmetric (anti-symmetric) at lower (higher) latitudes in meridional wind,

W1: anti-symmetric (symmetric) at lower latitudes and symmetric (anti-symmetric) at higher latitudes in temperature (zonal wind), and anti-symmetric in meridional wind,

S0: anti-symmetric in temperature and zonal wind and symmetric in meridional wind,

E1: anti-symmetric at lower and higher latitudes and symmetric at middle latitudes in temperature, anti-symmetric (symmetric) at lower (higher) latitudes in zonal wind, and meridional structure reversed the zonal structure, and

E2: symmetric (anti-symmetric) at lower (higher) latitudes in temperature and zonal wind, and meridional structure reversed the temperature and zonal wind.

Smaller amplitudes resulted in less confident phase structure for W4 and S0. The sum of all modes showed deviations from the W3 structure mainly due to W2 in the northern hemisphere, and to W2 and W1 (and possible E2 at higher latitudes) in the southern hemisphere.

Similar to Figure 6, Figure 7 shows horizontal structures of temperature and wind at 28 July 2012. Larger amplitudes were in the northern hemisphere for westward propagations in both temperature and wind, roughly increasing equatorward. For S0 and eastward propagations, amplitudes were larger in the southern hemisphere, maximizing at ~50°S. Probably because of small amplitudes, phases could not be determined with sufficient confidence. Among them, the W3 mode was anti-symmetric (symmetric) at lower (higher) latitudes and symmetric (anti-symmetric) at higher (lower) latitudes in temperature and zonal wind (meridional wind). Because W2 and E2 phases were similar at lower latitudes in the northern hemisphere, the sum in the northern hemisphere showed a mixture of W3, W2, and W1 at higher latitudes, and with E2 at lower latitudes. The southern hemisphere, on the other hand, exhibited slight deviations from W2 due to W1 and E1.

3.2. EP flux

Figure 8 shows latitude/altitude cross section of EP fluxes and divergence, as well as zonal mean zonal winds for each mode and the Q2DW on 22 January 2012. Note that W3, W2, and W1 exhibit similar flux structure at lower latitudes in the southern hemisphere, upward and poleward at <90 km and equatorward at higher altitudes. As with other features, E1 shows downward fluxes at lower latitudes and E2 shows upward and poleward fluxes at middle latitude and <100 km. Divergences are positive or small negative for all zonal wavenumbers, maximizing at lower latitudes and higher altitudes, except for at lower latitudes for W4, and at lower latitudes and high latitudes for W1.

Similar to Figure 8, Figure 9 shows the cross section for 28 July 2012. Clear features of fluxes are exhibited in W3 (upward and poleward at lower latitudes and altitudes), W2 (upward at lower altitudes and poleward at higher latitudes), and W1 (upward at higher latitudes). Q2DW fluxes, as sums of all modes, primarily reflect W3 fluxes. For W3 at lower latitudes, divergence is positive at lower altitudes and negative at higher altitudes.

3.3. Comparison of balance and radar winds

Figure 10 compares Q2DW meteor radar winds at six sites and MLS/balance winds at closest latitudes in January 2012. As a reference, W3 balance winds are also shown. Although radar data are available until 18 January at Bear Lake and until 15 January at Cerro Pachón, Q2DW winds agreed for the meridional component at Bear Lake and both components at Cerro Pachón. A different feature of these two sites is that phases of the balance wind Q2DW were modified from W3 by other modes at Bear Lake, which means that the W3 wind was not dominant in the Q2DW, while W3 and balance wind Q2DW agreed at Cerro Pachón. At Tierra del Fuego and Rothera, amplitudes of the balance wind Q2DW were larger than amplitudes of the W3 without changing phases. Amplitudes of the balance wind Q2DW were slightly smaller than radar amplitudes at Tierra del Fuego for both components but larger or equivalent at Rothera. However, phases agreed very well at the two sites for both components. These results are the same as those of Fritts et al. (2019). At Juliusruh, balance wind Q2DW differed from W3, and balance winds and radar winds agreed at the latter portion of the interval for the zonal component and were in reasonable agreement during the entire interval for the meridional component.

Similarly, Figure 11 compares radar and balance wind Q2DW in July 2012. The time series agreed best at Bear Lake. A W3 dominated the Q2DW, and they agreed with the radar in both amplitude and phase at the beginning (middle) of the interval for the zonal (meridional) component. Although amplitudes were larger in balance winds at the end of the interval for the zonal component, and in radar winds at the beginning and end of the interval for the meridional component, phases agreed for both components during the entire interval. Results at Juliusruh were similar to the results at Tierra del Fuego and Rothera in January, as shown in Figure 12. The W3 was dominant in the Q2DW, but balance wind amplitudes were smaller than radar amplitudes. However, phases agreed between the two. At Esrange, Tierra del Fuego, and Rothera, balance winds and radar winds did not agree in either amplitude or phase. As described in Fritts et al. (2019), the difference between radar and balance winds was large when short-term variations in amplitude or phase (period) were large, or when multiple modes equally contributed to the Q2DW. A possible primary reason for the disagreements is the coarse time resolution of 12 hours at a stage of Q2DW computations in the MLS geopotential height. Additionally, uncertainties of the Q2DW from observations were also large when its period was continuously away from 48 hours, e.g., close to 42 or 56 hours, because the Q2DWs were estimated by least-square fits to sinusoids with a period of 48 hours.

4. Discussion

Many Q2DW analyses used monthly mean amplitudes to study seasonal and interannual variabilities. Our 10-day mean W3 Q2DW employing MLS geopotential height and balance equations showed that maximum amplitudes of the meridional wind in January at 113 km and 40ºS were 35 ms^{-1} in 2010, 61 ms^{-1} in 2011, and 55 ms^{-1} in 2012, and monthly mean amplitudes were 19 ms^{-1}, 36 ms^{-1}, and 43 ms^{-1}, respectively. Larger monthly mean amplitudes for 2012 than 2011 is due to longer duration of enhancements in 2012. Half width half amplitudes were ~9, 11, and 15 days, respectively. In our analysis, mean amplitude of January at this location from 2010 to 2012 was ~35 ms^{-1}, but monthly mean amplitudes from data over multiple years are generally determined by creating a composite month. Our results showed that January mean amplitude from a composite month was reduced to ~60 % from the above value, due to phase variability.

To study correlations of the Q2DW in the MLT and at the stratosphere, we attempted Q2DW structure at lower altitudes between 30 and 60 km. Our results showed that the Q2DW was enhanced in winter with larger amplitudes in the southern hemisphere than the northern hemisphere. Maximum amplitudes were 8K at ~60°S and ~50 km in temperature, 60 ms^{-1} in the zonal wind and 70 ms^{-1} in the meridional wind at ~40°S and ~50 km for both components. Madhavi et al. (2015) studied structure of the stratospheric Q2DW at middle and high latitudes in both northern and southern hemispheres using Global Positioning Radio Occultation (GPSRO) Constellation Observing System for Meteorology, Ionosphere, and Climate (COSMIC) data during an interval from November 2006 to December 2010. They found enhancements in winter in both hemispheres with large interannual variability in amplitude. Limpasuvan et al. (2005) analyzed global structure of the Q2DW employing MLS data in water vapor, carbon monoxide, temperature and line-of-sight wind measurements from December 2004 to March 2005, and inferred that the Q2DW in the winter hemisphere is mainly trapped in the stratosphere and lower mesosphere. This implies a different generation mechanism of the Q2DW between the MLS and stratosphere.

Difference of the Q2DW between the stratosphere and MLT was also seen from vertical structure of our phase analyses. In January 2012 in the southern hemisphere, the W3 Q2DW in the MLT exhibited upward propagation with a vertical wavelength of ~110 km at 30ºS, longer poleward, and >200 km at 55ºS. In the stratosphere, on the other hand, the W3 Q2DW was downward propagation at ~30ºS. In July 2012, the W3 Q2DW showed downward propagation in the MLT and upward propagation in the stratosphere with vertical wavelengths of >100 km.

Q2DW responses at low and equatorial latitudes were analyzed employing ground-based radar data at Thumba (9°N, 77°E) from 2006 to 2009 by Babu et al. (2011), at Thumba and Kototabang (0°, 100°E) from 2006 to 2012 by Kumar et al. (2018), at Thumba from 2005 to 2014 and Tirunelveli (9°N, 78°E) from 1993 to 2009 by Rao et al. (2017), and at Kolhapur (17°N, 74°E) from 2013 to 2017 by Gaikwad et al. (2019). All of these researchers found amplitude enhancements in October, in addition to January and July. Particularly, Kumar et al. estimated primary zonal wavenumbers, that is, W3, W4, and W2 in January, July, and October, respectively. Lima et al. (2004) analyzed meteor radar data at Cachoeira Paulista (23°S, 45°W) from April 1992 to March 2002 and found enhancements only in summer and winter. Araújo et al. (2014), on the other hand, compared Q2DW responses at São João do Cariri (7°S, 37°W) with those at Cachoeira Paulista. Both summer and winter enhancements were observed at both sites, but enhancements were also observed in March and October only at São João do Cariri.

Our analyses poleward of 30° did not show any implications of Q2DW enhancements in October in both hemispheres, though the Q2DW was enhanced from late April to early May but only in the southern hemisphere. This implies that the Q2DW can be generated moderately in austral autumn at equatorial latitudes and propagate poleward in the southern hemisphere but not in the northern hemisphere and the Q2DW in boreal autumn is only an equatorial phenomenon.

Gurubaran et al. (2001b) reported Q2DW responses stronger in winter than summer at Tirunelveli. If the Q2DW is generated in the summer hemisphere and propagates to the winter hemisphere (Craig et al., 1983; Rao et al., 2017), this suggests that Q2DW responses at Tirunelveli are larger when propagated from the summer southern hemisphere than generated in the summer northern hemisphere. Nozawa et al. (2003a, 2003b) analyzed Q2DW employing MF radar wind measurements at Tromsø (70°N, 19°E) and Poker Flat (65°N, 148°W) from 1998 to 2002 and found stronger responses in winter. Tunbridge and Mitchell (2009) found significant interannual variability of Q2DW responses from meteor radar wind measurements at Esrange (68°N, 21°E), which is close to Tromsø, from 1999 to 2008. According to Tunbridge and Mitchell, summer amplitudes were much larger than amplitudes in January and February in 2000, 2002, 2003, 2005, and 2007, and winter amplitudes were equal to or greater than summer amplitudes in 2004 and 2006. Specifically, their observations revealed that Q2DW responses from late November 2007 to late January 2008 were stronger than responses in July 2007 and 2008. It is unclear yet about interannual variabilities of Q2DW amplitudes. But as a plausible reason, because the Q2DW is a superposition of different zonal wavenumbers in the northern hemisphere (Ern et al., 2013), amplitudes of each zonal wavenumber may have significant seasonal and interannual variabilities. From a ground measurement at a single site, it is impossible to estimate amplitudes of zonal wavenumbers. As seen in Figure 7, when multiple zonal wavenumbers contribute to the Q2DW, there is a longitudinal variability by a superposition. Our results showed that the W3 maximized in July in the northern hemisphere, and W3 amplitudes were comparable to other zonal wavenumbers in January. Q2DW amplitudes in January are incited when different zonal wavenumbers are inphase and suppressed when they are anti-phase.

It is well known that Q2DW responses in summer are larger in the southern hemisphere than the northern hemisphere and W3 dominates the summer Q2DW in the southern hemisphere. If planetary waves are sensitive to background conditions, difference of zonal mean zonal winds between the hemispheres may cause the difference of the W3 Q2DW responses. Zonal mean zonal winds inferred from MLS/balance equations showed <10 ms^{-1} between 90 and 110 km in the summer southern hemisphere at lower latitudes, and larger eastward winds at ~90 km and westward winds at >100 km in the summer northern hemisphere than the summer southern hemisphere. Therefore, altitude and latitude variabilities of the zonal wind zonal winds at lower latitudes were larger in the northern hemisphere. However, westward acceleration at lower latitudes was larger in the southern hemisphere, especially at higher altitudes. Additionally, day-to-day variability of zonal mean temperature was also larger in the summer southern hemisphere than the northern hemisphere.

Planetary waves are expected to be enhanced at baroclinic/barotropic instabilities. A necessary condition for the instabilities is the meridional gradient of the quasi-geostrophic potential vorticity (q_ϕ) < 0 (Liu et al., 2004; Yue et al., 2012a), which is derived from an equation

$$q_\phi = 2\Omega \cos\phi - [(\bar{u} \cos\phi)_\phi / (a \cos\phi)]_\phi - a/\rho\, [(f^2 / N_2)\, \rho\, \bar{u}_z]_z, \qquad (8)$$

where N is Brunt-Väisälä frequency, and ρ is density. We obtained $q_\phi < 0$ in January only at 40ºS and < 80 km and at 70ºS and >105 km, agreeing with Gu et al. (2016) and Liu et al. (2004), but $q_\phi > 0$ in the July northern hemisphere. According to equation (8), the sum of the second and third terms must be greater than the first term for $q_\phi < 0$. However, both second and third terms are negative, except for >110 km at high latitudes and <80 km at ~40ºS.

The second term in the meridional component of the EP flux equation (Equation 6) was larger by ~20 times than the first term at 102 km in the January in the southern hemisphere. Therefore, the meridional component primarily depends on u' and v' amplitudes. Amplitudes of the meridional component were ~4 times larger in January in the southern hemisphere than in July in the northern hemisphere. Meridional fluxes were positively large at higher altitudes increasing equatorward with a maximum of >1300 m^2s^{-2} in January in the southern hemisphere, but fluxes were positive at lower altitudes with a maximum of >80 m^2s^{-2} and negative at higher altitudes with a minimum of <–200 m^2s^{-2} in July in the northern hemisphere, with equivalent positive values at high latitudes in the southern hemisphere.

Vertical winds at local sites were measured by meteor radars (Egito et al., 2016; Eswaraiah et al., 2011) and reported up to a few 10 ms^{-1}. According to Yajnavalkya and Andrew (2010), vertical winds are sum of meridional circulation, geomagnetic activity, and residual influence by short-period waves, such as gravity waves and tides and the vertical winds in the meridional circulation are expected to be in the order of cms^{-1} (Portnyagin et al., 2010). We expected the third term of the altitude component (Equation 7) to be negligible. Therefore, the altitude component primarily depends on structures of geopotential height and meridional wind. Structures of the altitude component of EP fluxes were similar between January in the southern hemisphere and July in the northern hemisphere, but ~8 times larger in magnitude in January in the southern hemisphere.

Fritts et al. (2019) showed EP fluxes for each zonal wavenumber in the southern hemisphere on three days in January 2015. Their results for W3 and W1 on 22 January 2015 are very similar to ours (as shown in Figure 8). For W2, large upward and poleward fluxes at high latitudes were exhibited by Fritts et al., while our results maximized at lower latitudes. Magnitudes for fluxes were larger in our results than those of Fritts et al., but this is not surprising because Q2DW amplitudes in January in the southern hemisphere were larger in 2012 than 2015. Gu et al. (2016) derived EP fluxes of the Q2DW in the northern hemisphere during boreal summer in 2007 employing ensemble data assimilation version of the Whole Atmosphere Community Climate Model + Data Assimilation Research Testbed. Their W3 EP flux structure shows upward and poleward fluxes at lower latitudes and lower altitudes and equatorward fluxes at higher altitudes. Overall structure agrees with our results although qualitative difference exists probably due to interannual variabilities. To continue this work, we plan to study interannual variabilities of Q2DW structure and EP fluxes further.

5. Summary

We compared structure and variability of the Q2DW in temperature and horizontal winds for summer and winter between the northern and southern hemispheres, employing balance equations with Aura/MLS temperature and geopotential height data at latitudes between 30 and 70º and altitudes between 70 and 120 km. For the comparison, January and July 2012 were chosen due to larger mean amplitudes and longer enhancement durations than other years.

Q2DW amplitudes increased with altitude in the MLT, maximizing in summer in both hemispheres. Summer amplitudes maximized at lower latitudes, decreasing poleward. Amplitudes in summer increased with altitude while amplitudes in winter maximized at ~90 km. Enhancements in January in the southern hemisphere were dominated by W3, as previously reported, but a mixture with other modes comprised the Q2DW in the northern hemisphere and the winter southern hemisphere although maximum amplitudes were W3. Therefore, Q2DW wind fields had large longitudinal variabilities in winter southern hemisphere and summer and winter northern hemisphere, although longitudinal structure of the summer Q2DW in the southern hemisphere was a distortion from W3. The W3 Q2DW in January was anti-symmetric with respect to the equator at middle and high latitudes in temperature and zonal wind, and symmetric at middle latitudes in meridional wind.

The meridional component of EP fluxes maximized equatorward at ~ 110 km and the altitude component of EP fluxes maximized between 80 and 90 km in both summer and winter in both hemispheres. EP fluxes in summer differed between the hemispheres. In the southern hemisphere, structures of W3 and W1 were similar, that is, upward at lower altitudes and equatorward at higher altitudes at lower latitudes, upward at lower and middle latitudes for W2 and at middle latitudes for E2, and downward at lower latitudes for E1. In the northern hemisphere, EP fluxes were upward and poleward at lower latitudes for W3 and middle-to-high latitudes for W1, toward ~90 km and 60°N for W2.

SkiYMet at three sites in each hemisphere was operating in January and July 2012, and the Q2DW was compared between meteor radar wind measurements and balance wind. Results agreed in the summer southern hemisphere and lower latitude sites in the northern and winter southern hemispheres. Disagreements were larger in phases when amplitudes were smaller and also large when multiple zonal wavenumber modes comprised the Q2DW or when Q2DW amplitudes or periods changed largely in a short-timeframe.

Acknowledgements

Research described here was funded by NSF and NASA grants cited in GEMS. We also thank the EARG personnel for their invaluable help with the operation of SAAMER. We are also very grateful for the invaluable support of Jorge L. Chau and Gunter Stober at the University of Rostock, and Fabio A. Vargas at University of Illinoi. MLS data are available online (https://mls.jpl.nasa.gov/index-eos-mls.php). Meteor radar data used here are available online (http://cedar.openmadrigal.org).

Reference

Araújo, L. R., Lima, L. M., Batista, P. P., Clemesha, B. R., and Takahashi, H. (2014), Planetary wave seasonality from meteor wind measurements at 7.4°S and 22.7°S, *Ann. Geophys.*, 32(5), 519-531, doi:10.5194/angeo-32-519-2014.

Azeem, S. M. I., Palo, S. E., Wu, D. L., and Froidevaux, L. (2001), Observations of the 2-Day Wave in UARS MLS Temperature and Ozone Measurements, *Geophys. Res. Lett.*, 28(16), 3147-3150, doi:10.1029/2001GL013119.

Babu, V. S., Kumar, K. K., John, S. R., Subramanyam, K. V., and Ramkumar, G. (2011), Meteor radar observations of short-term variability of quasi 2 day waves and their interaction with tides and planetary waves in mesosphere-lower thermosphere region over Thumba (8.5°N, 77°E), *J. Geophys. Res.*, 116, D16121, doi:10.1029/2010JD015390.

Baumgaertner, A. J. G., McDonald, A. J., Hibbins, R. E., Fritts, D. C., Murphy, D. J., and Vincent, R. A. (2008), Short-period planetary waves in the Antarctic middle atmosphere, *J. Atmos. Sol.-Terr. Phys.*, 70, 1336-1350, doi:10.1016/j.jastp.2008.04.007.

Bristow, W. A., Yee, J.-H., Zhu, X., and Greenwald, R. A. (1999), Simultaneous observations of the July 1996 2-day wave event using the Super Dual Auroral Radar Network and the High Resolution Doppler Imager, *J. Geophys. Res.*, 104(A6), 12,715-12,721, doi:10.1029/1999JA9000030.

Chshyolkova, T., Manson, A. H., and Meek, C. E. (2005), Climatology of the quasi two-day wave over Saskatoon (52°N, 107°W): 14 Years of MF radar observations, *Adv. Space Res.*, 35(11), 2011-2016, doi:10.1016/j.asr.2005.03.040.

Craig, R. L., and Elford, W. G. (1981), Observations of the quasi 2-day wave near 90 km altitude at Adelaide (35°S), *J. Atmos. Terr. Phys.*, 43(10), 1051-1056, doi:10.1016/0021-9169(81)90019-2.

Craig, R. L., Vincent, R. A., Fraser, G. J., and Smith, M. J. (1980), The quasi 2-day wave in the Southern Hemisphere mesosphere, *Nature*, 287, 319-320, doi:10.1038/287319aO.

Craig, R. L., Vincent, R. A., Kingsley, S. P., and Muller, H. G. (1983), Simultaneous observations of the quasi 2-day wave in the northern and southern hemispheres, *J. Atmos. Terr. Phys.*, 45(8-9), 539-541, doi:10.1016/S0021-9169(83)80068-3.

Egito, F., Andrioli, V. F., and Batista, P. P. (2016), Vertical winds and momentum fluxes due to equatorial planetary scale waves using all-sky meteor radar over Brazilian region, *J. Atmos.-Sol. Terr. Phys.*, 149, 108-119, doi:10.1016/j.jastp.2016.10.005.

Eswaraiah, S., Ratnam, M. V., Murthy, B. V. K., and Rao, S. V. B. (2011), Low-latitude mesospheric vertical winds observed using VHF radar, *J. Geophys. Res.*, 116, D22117, doi:10.1029/2011JD016385.

Ern, M., Preusse, P., Kalisch, S., Kaufmann, M., and Riese, M. (2013), Role of gravity waves in the forcing of quasi two-day waves in the mesosphere: An observational study, *J. Geophys. Res.* (*Atmos.*), 118(9), 3467-3485, doi:10.1029/2012JD018208.

Fritts, D. C., Isler, J. R., Lieberman, R. S., Burrage, M. D., Marsh, D. R., Nakamura, T., Tsuda, T., Vincent, R. A., and Reid, I. M. (1999), Two-day wave structure and mean flow interactions observed by radar and High Resolution Doppler Imager, *J. Geophys. Res.*, 104(D4), 3953-3969, doi:10.1029/1998JD200024.

Gaikwad, H. P., Sharma, A. K., Gurav, O. B., Chavan, G. A., Nade, D. P., Patil, P. T., Nikte, S. S., and Naniwadekar, G. P. (2019), Seasonal, annual, and interannual variability in MLT quasi-two-day waves over the low-latitude region Kolhapur (16.8°N; 74.2°E), *Adv. Space Res.*, 63(7), 2100-2117, doi:10.1016/j.asr.2018.12.029.

Gu, S.-Y., Li, T., Dou, X. Wu, Q., Mlynczak, M. G., and Russell, J. M. (2013), Observations of Quasi-Two-Day wave by TIMED/SABER and TIMED/TIDI, *J. Geophys. Res.* (*Atmos.*), 118(4), 1624-1639, doi:10.1002/jgrd.50191.

Gu, S.-Y., Liu, H.-L., Pedatella, N. M., Dou, X., and Shu, Z. (2016), The quai-2 day wave activities during 2007 boreal summer period as revealed by Whole Atmosphere Community Climate Model, *J. Geophys. Res.* (*Space Phys.*), 121(7), 7256-7268, doi:10.1002/2016JA022867.

Guharay, A., Batista, P. P., Clemesha, B. R., and Schuch, N. J. (2013), Study of the quasi-two-day wave during summer over Santa Maria, Brasil using meteor radar observations, *J. Atmos. Sol.-Terr. Phys.*, 92, 83-93, doi:10.1016/j.jastp.2012.10.005.

Gurubaran, S., Ramkumar, T. K., Sridharan, S., and Rajaram, R. (2001a), Signatures of quasi-2-day planetary waves in the equatorial electrojet: results from simultaneous observations of mesospheric winds and geomagnetic field variations at low latitudes, *J. Atmos. Sol.-Terr. Phys.*, 63(9), 813-821, doi:20.1016/6826(00)00193-0.

Gurubaran, S., Sridharan, S., Ramkumar, T. K., and Rajaram, R. (2001b), The mesospheric quasi-2-day wave over Tirunelveli (8.7°N), *J. Atmos. Sol.-Terr. Phys.*, 63, 975-985, doi:10.1016/S1364-6826(01)00016-5.

Hagan, M. E., Forbes, J. M., and Vial, F. (1993), Numerical Investigation of the Propagation of the Quai-Two-Day Wave Into the Lower Thermosphere, *J. Geophys. Res.*, 98(D12), 23,193-23,205, doi:10.1029/93JD02779.

Harris, T. J. (1994), A long-term study of the quasi-two-day wave in the middle atmosphere, *J. Atmos. Terr. Phys.*, 56(5), 569-579, doi:10.1016/0021-9169(94)90098-1.

Harris, T. J., and Vincent, R. A. (1993), The Quasi-Two-Day Wave Observed in the Equatorial Middle Atmosphere, *J. Geophys. Res.*, 98(D6), 10,481-10,490, doi:10.1029/93JD00380.

Hecht, J. H., Walterscheid, R. L., Gelinas, L. J., Vincent, R. A., Reid, I. M., and Woithe, J. M. (2010), Observations of the phase-locked 2 day wave over Australian sector using medium-frequency radar and airglow data, *J. Geophys. Res.*, 115, D16115, doi:10.1029/2009JD013772.

Huang, Y. Y., Zhang, S. D., Yi, F., Huang, C. M., Huang, K. M., Gan, Q., and Gong, Y. (2013), Global climatological variability of quasi-two-day waves revealed by TIMED/SABER observations, *Ann. Geophys.*, 31, 2061-1075, doi:10.5194/angeo-31-1061-2013.

Hunt, B. G. (1981), The 2-day wave in the middle atmosphere as simulated in a general circulation model extending from the surface to 100 km, *J. Atmos. Terr. Phys.*, 43(11), 1143-1154, doi:10.1016/0021-9169(81)90030-1.

Jacobi, Ch., Schminder, R., and Kürschner, D. (1997), The quasi 2-day wave as seen from D1 LF wind measurements over Central Europe (52°N, 15°E) at Collm, *J. Atmos. Sol.-Terr. Phys.*, 59(11), 1277-1286, doi:10.1016/S1364-6826(96)00170-8.

Jacobi, Ch., Schminder, R., and Kürschner, D. (1998), Non-linear interaction of the quasi 2-day wave and long-term oscillations in the summer midlatitude mesopause region as seen from LF D1 wind measurements over Central Europe (Collm, 52°N, 15°E), *J. Atmos. Sol.-Terr. Phys.*, 60(12), 1175-1191, doi:10.1016/S1364-6826(98)00076-5.

Jia, Y., Liu, H.-L., and Change, L. C. (2012), Numerical investigation of the quasi 2 day wave in the mesosphere and lower thermosphere, *J. Geophys. Res. Atmos.*, 117, D05111, doi:10.1029/2011JD016574.

Kulikov, M. Y. (2007), Theoretical investigation of the influence of a quasi-2-day wave on nonlinear photochemical oscillations in the mesopause region, *J. Geophys. Res.*, 112, D02305, doi:10.1029/2005JD006845.

Kumar, K. K., Subrahmanyam, K. V., Mathew, S. S., Koushik, N., and Ramkumar, G. (2018), Simultaneous observations of the quasi 2-day wave climatology over the low and equatorial latitudes in the mesosphere lower thermosphere, *Clim. Dyn.*, 51, 221-233, doi:10.1007/s00382-01703916.2.

Li, T., She, C.-Y., Palo, S. E., Wu, Q., Liu, H.-L., and Salby, M. L. (2008), Coordinated lidar and TIMED observations of the quasi-two-day wave during August 2002-2004 and possible quasi-biennial oscillation influence, *Adv. Space Res.*, 41(9), 1463-1471, doi:10.1016/j.asr.2007.03.052.

Lieberman, R. S. (1999), Eliassen-Palm Fluxes of the 2-Dat Wave, *J. Atmos. Sci.*, 56(16), 2846-2861, doi:10.1175/1520-0469(1999)-56<2846:EPFOTD>2.0.CO;2.

Lima, L., Alves, M. E. O., Batista, P. P., Clemesha, B. R., Medeiros, A. F., and Buriti, R. A. (2012), Sudden stratospheric warming effects on the mesospheric tides and 2-day wave dynamics at 7°S, *J. Atmos. Sol.-Terr. Phys.*, 78-79, 99-107, doi:10.1019/j.jastp.2011.02.013.

Lima, L. M., Batista, P. P., Takahashi, H., and Clemesha, B. R. (2004), Quasi-two-day wave observed by meteor radar at 22.7°S, *J. Atmos. Sol.-Terr. Phys.*, 66(6-9), 529-537, doi:10.1016/j.jastp.2004.01.007.

Limpasuvan, V., and Dong, W. L. (2009), Anomalous two-day wave behavior during the 2006 austral summer, *Geophys. Res. Lett.*, 36(4), L04807, doi:10.1029/2008GL036387.

Limpasuvan, V., Wu, D. L., Schwartz, M. J., Waters, J. W., Wu, Q., and Killeen, T. L. (2005), The two-day wave in EOS MLS temperature and wind measurements during 2004-2005 winter, *Geophys. Res. Lett.*, 32(17), L17809, doi:10.1029/2005GL023396.

Limpasuvan, V., and Wu, D. L. (2009), Anomalous two-day wave behavior during the 2006 austral summer, *Geophys. Res. Lett.*, 36(4), L04807, doi:10.1029/2008GL036387.

Limpasuvan, V., and Wu, D. L. (2003), Two-day wave Observations of UARS Microwave Limb Sounder mesospheric water vapor and temperature, *J. Geophys. Res.*, 108(D19), ACL 4-1, 4307, doi:10.1029/2002JD002903.

Liu, H.-L., Talaat, E. R., Roble, R. G., Lieberman, R. S., Riggin, D. M., and Yee, J.-H. (2004), The 6.5-day wave and its seasonal variability in the middle and upper atmosphere, *J. Geophys. Res.*, 109(D21), D21112, doi:10.1029/2004JD004795.

Madhavi, G. N., Kishore, P., Rao, S. V. B., Velicogna, I., and Basha, G. (2015), Two-day wave observations over the middle and high latitudes in the NH and SH using COSMIC GPSRO measurements, *Adv. Space. Res.*, 55(2), 722-731, doi:10.1016/j.asr.2014.09.032.

Malinga, S. B., and Ruohoniemi, J. M. (2007), The quasi-two-day wave studied using the northern hemisphere SuperDARN HF radars, *Ann. Geophys.*, 25(8), 1767-1778, doi:10.5194/angeo-25-1767-2007.

Meek, C. E., Manson, A. H., Franke, S. J., Singer, W., Hoffmann, P., Clark, R. R., Tsuda, T., Nakamura, T., Tsutsumi, M., Hagan, M., Fritts, D. C., Isler, J., and Portnyagin, Yu. I. (1996), Global study of northern hemisphere quasi-2-day wave events in recent summers near 90 km altitude, *J. Atmos. Terr. Phys.*, 58(13), 1401-1411,doi:10.1016/0021-9169(95)00120-4.

Merzlyakov, E., Pancheva, D., Mitchell, N., Forbes, J. M., Portnyagin, Yu. I., Palo, S., Makarov, N., and Muller, H. G. (2004), High- and mid-latitude quasi-2-day waves observed simultaneously by four meteor radars during summer 2000, *Ann. Geophys.*, 22(3), 773-788, doi:10.5194/angeo-22-1917-2004.

Merzlyakov, E. G., and Jacobi, Ch. (2004), Quasi-two-day wave in an unstable summer atmosphere – some numerical results on excitation and propagation, *Ann. Geophys.*, 22(6), 1917-1929, doi:10.5194/angeo-22-1917-2004.

Morris, R. J., Klekouciuk, A. R., and Holdsworth, D. A. (2009), Low latitude 2-day planetary wave impact on austral polar mesopause temperatures: revealed by a January diminution in PMSE above Davis, Antarctica, *Geophys. Res. Lett.*, 36, L11807, doi:10.1029/2009GL037817.

Murphy, D. J., and Vincent, R. A. (1998), Mesospheric momentum fluxes over Adelaide during the 2-day wave: Results and interpretation, *J. Geophys. Res.*, 103(D22), 28,627-28,636, doi:10.1029/1998JD2000001.

Namboothiri, S. P., Kishore, P., and Igarashi, K. (2002), Observations of the quasi-2-day wave in the mesosphere and lower thermosphere over Yamagawa and Wakkanai, *J. Geophys. Res.* (*Atmos.*), 17(D16), 4320, doi:10.1029/2001JD000539.

Nozawa, S., Imaida, S., Brekke, A., Hall, C. M., Manson, A., Meek, C., Oyama, S., Dobashi, K., and Fujii, R. (2003a), The quasi 2-day wave observed in the polar mesosphere, *J. Geophys. Res.*, 108(D2), 4039, doi:10.1029/2002JD002440.

Nozawa, S., Iwahashi, H., Brekke, A., Hall, C. M., Meek, C., Manson, A., Oyama, S., Murayama, Y., and Fujii, R. (2003b), The quasi 2-day wave observed in the polar mesosphere: Comparison of the characteristics observed at Tromsø and Poker Flat, *J. Geophys. Res.*, 108(D24), 4748, doi:10.1029/2002JD003221.

Offermann, D., Hoffmann, P., Knieling, P., Koppmann, R., Oberheide, J., Riggin, D. M., Tunbridge, V. M., and Steinbrecht, W. (2001), Quasi 2 day waves in the summer mesosphere: Triple structure of amplitudes and long-term development, *J. Geophys. Res.*, 116, D00P02, doi:10.1029/2010JD015051.

Pancheva, D. V., Mukhtarov, P. J., Shepherd, M. G., Mitchell, N. J., Fritts, D. C., Riggin, D. M., Franke, S. J., Batista, P. P., Abdu, M. A., Batista, I. S., Clemesha, B. R., and Kikuchi, T. (2006), Two-day wave coupling of the low-latitude atmosphere-ionosphere system, *J. Geophys. Res.*, 111, A07313, doi:10.1029/2005JA011562.

Pancheva, D., Mitchell, N. J., Manson, A. H., Meek, C. E., Jacobi, Ch., Portnyagin, Yu., Merzlyakov, E., Hocking, W. K., MacDougall, J., Singer, W., Igarashi, K., Clark, R. R., Riggin, D. M., Franke, S. J., Kürschener, D., Fahrutdinova, A. N., Stepanov, A. M., Kashcheyev, B. L., Oleynikov, A. N., and Muller, H. G. (2004), Variability of the quasi-2-day wave observed in the MLT region during the PSMOS campaign of June-August 1999, *J. Atmos. Sol.-Terr. Phys.*, 66(6-9), 539-365, doi:10.1016/j.jastp.2004.01.008.

Pedatella, N. M., and Forbes, J. M. (2012), The quasi 2 day wave and spatial-temporal variability of the OH emission and ionosphere, *J. Geophys. Res.*, 117, A01320, doi:10.1029/2011JA017186.

Pendlebury, D. (2012), A simulation of the quasi-two-day wave and its effect on variability of summertime mesopause temperatures, *J. Atmos. Sol.-Terr. Phys.*, 80, 138-151, doi:10.1016/j.jastp.2012.01.006.

Pfister, L. (1985), Baroclinic Instability of Easterly Jets with Applications to the Summer Mesosphere, *J. Atmos. Sci.*, 42(4), 313-330, doi:10.1175/1520-0469(1985)042<0313:BIOEJW>2.0.CO;2.

Plumb, R. A. (1983), Baroclinic Instability of the Summer Mesosphere: A Mechanism for the Quasi-Two-Day Wave? *J. Atmos. Sci.*, 40(1), 262-270, doi:10.1175/1520-0469(1983)040<0262:BIOTSM>2.0.CO;2.

Poole, L. M. G. (1990), The characteristics of the mesospheric two-day wave as observed at Grahamstown (33.3°S, 26.5°E), *J. Atmos. Terr. Phys.*, 52(4), 259-268, doi:10.1016/0021-9169(90)90093-3.

Poole, L. M. G., and Harris, T. J.s (1995), The propagation of the mesospheric two-day wave in the southern hemisphere, *J. Atmos. Terr. Phys.*, 57(13), 1661-1666, doi:10.1016/0021-9169(95)98845-3.

Portnyagin, Yu. I., Solov'era, T. V., Merzlyakov, E. G., Pogorel'tsev, A. I., and Savenkova, E. N. (2010), Height-Latitude Structure of the Vertical Wind in the Upper Mesosphere and Lower Thermisphere (70 – 110 km), *Izvestiya, Atmos. Ocean. Phys.*, 46(1), 85-94, doi:10.1134/S0001433811010117.

Rao, N. V., Ratnam, M. V., Vedavathi, C., Tsuda, T., Murthy, B. V. K., Sathishkumar, S., Gurubaran, S., Kumar, K. K., Subrahmanyam, K. V., and Rao, S. V. B. (2017), Seasonal, inter-annual and solar cycle variability of the quasi two day wave in the low-latitude mesosphere and lower thermosphere, *J. Atmos. Sol.-Terr. Phys.*, 152, 20-29, doi:10.1016/j.jastp.2016.11.005.

Riggin, D. A., Lieberman, R. S., Vincent, R. A., Manson, A. H., Meek, C. E., Nakamura, T., Tsuda, T., and Portnyagin, Yu. I. (2004), The 2-day wave during the boreal summer of 1994, *J. Geophys. Res.*, 109, D08110, doi:10.1029/2003JD004493.

Rodgers, C. D., and Prata, A. J. (1981), The quasi 2 day wave and spatial-temporal variability of the OH emission and Ionosphere, *J. Geophys. Res.*, 117, A01320, doi:10.1029/2011JA017186.

Rojas, M., and Norton, W. (2007), Amplification of the 2-day wave from mutual interaction of global Rossby-gravity and local modes in the summer mesosphere, *J. Geophys. Res.*, 112, D12114, doi:10.1029/2006JD008084.

Salby, M. L. (1980), The influence of Realistic Dissipation on Planetary Normal Structures, *J. Atmos. Sci.*, 37(10), 2186-2199, doi:10.1175/1520-0469(1980)037<2186.TIORDO>2.0.CO;2.

Salby, M. L. (1981a), Rossby Normal Modes in Nonuniform Background Configurations. Part I. Simple Fields, *J. Atmos. Sci.*, 38(9), 1803-1804, doi:10.1175/1520-0469(1981)038<1803:RNMINB>2.0.CO;2.

Salby, M. L. (1981b), Rossby Normal Modes in Nonuniform Background Configurations. Part II. Equinox and Solstice Conditions, *J. Atmos. Sci.*, 38(9), 1827-1840, doi:10.11751520-0469(1981)038<1827:RNMINB>2.0.CO;2.

Salby, M. L. (1981c), The 2-Day Wave in the Middle Atmosphere: Observations and Theory, *J. Geophys. Res.*, 86(C10), 9654-9660, doi:10.1029/JC086iC10p09654.

Salby, M. L., and Callaghan, P. F. (2003), Dynamics of the 2-day wave in a nonlinear model of the middle and upper atmosphere, *J. Geophys. Res.*, 108(D23), 4713, doi:10.1029/2003JD003648.

Salby, M. L., and Callaghan, P. F. (2001), Seasonal Amplification of the 2-Day Wave: Relationship between Normal Mode and Instability, *J. Atmos. Sci.*, 58(14), 1858-1869, doi:10.1175/1520-0469(2001)058<1858:SAOTDW>2.0.CO;2.

Sandford, D. J., Schwartz, M. J., and Mitchell, N. J. (2008), The wintertime two-day wave in the polar stratosphere, mesosphere and lower thermosphere, *Atmos. Chem. Phys.*, 8(3), 749-755, doi:10.5194/acp-8-749-2008.

Schröder, H., and Schmitz, G. (2004), A generation mechanism for the 2-day wave near the stratopause: Mixed barotropic inertial instability, *J. Geophys. Res.*, 109, D24116, doi:10.1029/2004JD005177.

Sonnemann, G. R., and Grygalashbyly, M. (2005), On the two-day oscillations and the day-to-day variability in global 3-D-modeling of the chemical system of the upper mesosphere/mesopause region, *Nonlin. Proc. Geophys.*, 12(5), 691-705, doi:10.5194/npg-12-691-2005.

Takahashi, H., Lima, L. M., Wrasse, C. M., Batista, I. S., Onohara, A., Aquino, M. G. S., Batista, P. P., and Abdu, M. A. (2012), Ionospheric response to 2-day planetary wave in the equatorial and low latitude regions, *J. Atmos. Sol.-Terr. Phys.*, 90, 164-171, doi:10.1016/j.jastp.2012.04.006.

Thayaparan, T., Hocking, W. K., and MacDougall, J. (1997a), Amplitude, phase, and period variations of the quasi 2-day wave in the mesosphere and lower thermosphere over London, Canada (43°N, 81°W), during 1993 and 1994, *J. Geophys. Res.*, 102(D8), 9461-9478, doi:10.1029/96JD03869.

Thayaparan, T., Hocking, W. K., MacDougall, J., Manson, A. H., and Meek, C. E. (1997b), Simultaneous observations of the 2-day wave at London (43°N, 81°W) and Saskatoon (52°N, 107°W) near 91 km altitude during the two years of 1993 and 1994, *Ann. Geophys.*, 15(10), 1324-1339, doi:10.1007/s00585-997-1324-3.

Tsuda, T., Kato, S., and Vincent, R. A. (1988), Long-period wind oscillations observed by the Kyoto meteor radar and comparison of the quasi-2-day wave with Adelaide HF radar observations, *J. Atmos. Terr. Phys.*, 50(3), 225-230, doi:10.1016/0021-9169(88)90071-2.

Tunbridge, V. M., and Mitchell, N. J. (2009), The two-day wave in the Antarctic and Arctic mesosphere and lower thermosphere, *Atmos. Chem. Phys.*, 9(17), 6377-6388, doi:10.5194/acp-9-6377-2009.

Tunbridge, V. M., Sandford, D. J., and Mitchell, N. J. (2011), Zonal wavenumber of the summertime 2 day planetary wave observed in the mesosphere by EOS Aura Microwave Limb Sounder, *J. Geophys. Res.*, 116, D11103, doi:10.1029/2010JD014567.

Ward, W. E., Wang, D. Y., Solheim, B. H., and Shepherd, G. G. (1996), Observations of the two-day wave in WINDII data during January, 1993, *Geophys. Res. Lett.*, 23(21), 2923-2936, doi:10.1029/96GL02897.

Wu, D. L., Fishben, E. F., Read, W. G., and Waters, J. W. (1996), Excitation and Evolution of the Quasi-2-Day Wave Observed in UARS/MLS Temperature Measurements, *J. Atmos. Sci.*, 53(5), 728-738, doi:10.1175/1520-0469(1996)053<0728:EAEOTQ>2.0.CO;2.

Wu, D. L., Hays, P. B., Skinner, W. R., Marshall, A. R., Burrage, M. D., Lieberman, R. S., and Ortland, D. A. (1993), Observations of the quasi 2-day wave from the High Resolution Doppler Imager on UARS, *Geophys. Res. Lett.*, 20(24), 2853-2856, doi:10.0129/93GL03008.

Yajnavalkoya, B., and Gerrand, A. J. (2010), Wintertime mesopause region vertical winds from Resolute Bay (2010), *J. Geophys. Res.*, 115, D00N07, doi:10.1029/2010JD014113.

Yue, J., H.-L. Liu, and Chang, L. C. (2012a), Numerical investigation of the quasi 2 day wave in the mesosphere and lower thermosphere, J. Geophys. Res., 117, D05111, doi:10.1029/2011JD016574.

Yue, J., Wang, W., Richmond, A. D., and Liu, H.-L. (2012b), Quasi-two-day wave coupling of the mesosphere and lower thermosphere-ionosphere in the TIME-GCM: Two-day oscillations in the ionosphere, *J. Geophys. Res.*, 117, A07305, doi:10.1029/2012JA017815.

Figures

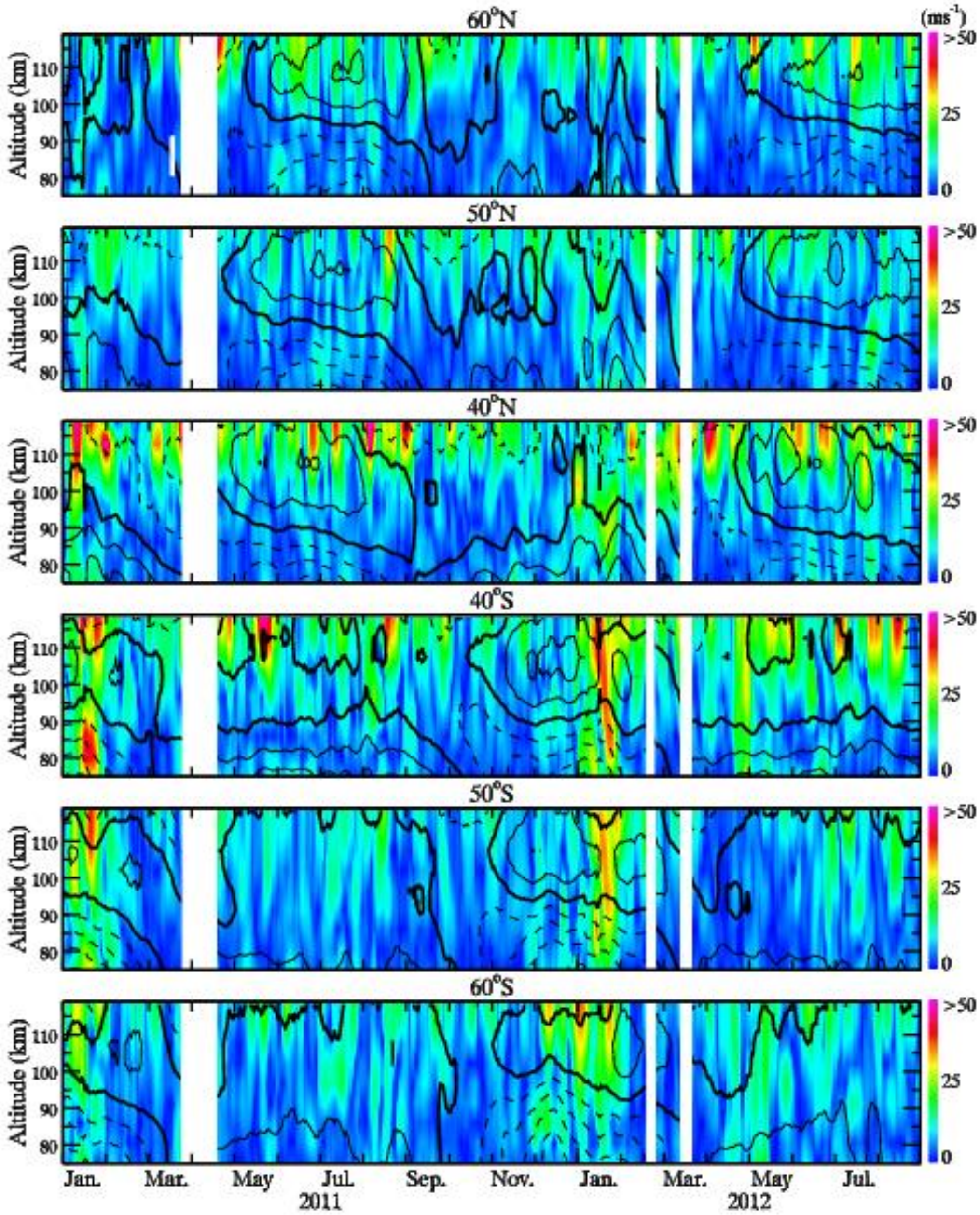

Figure 1. Q2DW amplitudes of the zonal component induced by MLS balance equation as functions of altitude from January 2011 to August 2012 at 60°N, 50°N, 40°N, 40°S, 50°S, and 60°S from top to bottom. Line contours indicate zonal mean zonal winds every 20 ms^{-1}. Thick lines indicate 0 ms^{-1} and solid and dashed lines are eastward and westward.

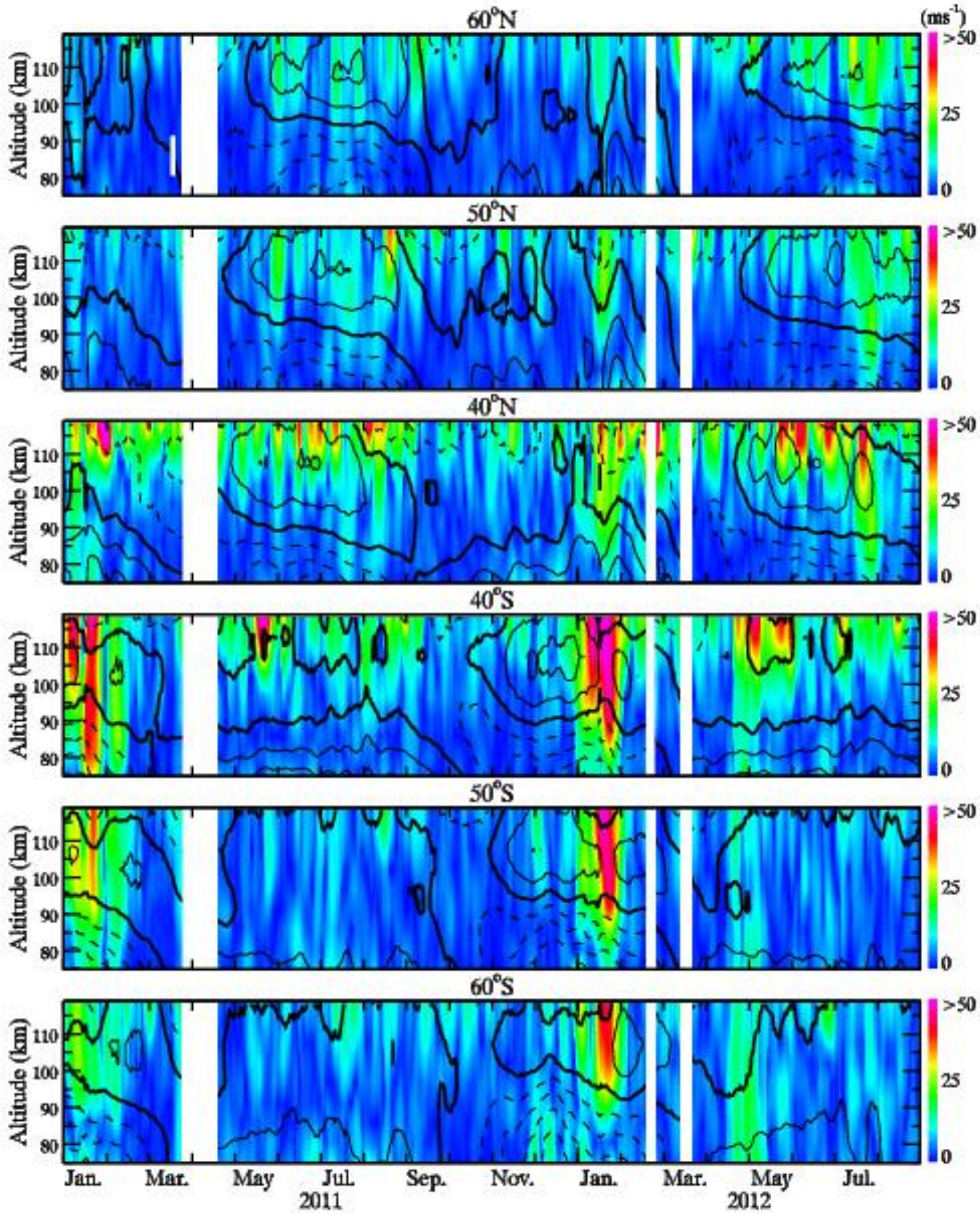

Figure 2. Same as Figure 1, but for meridional component.

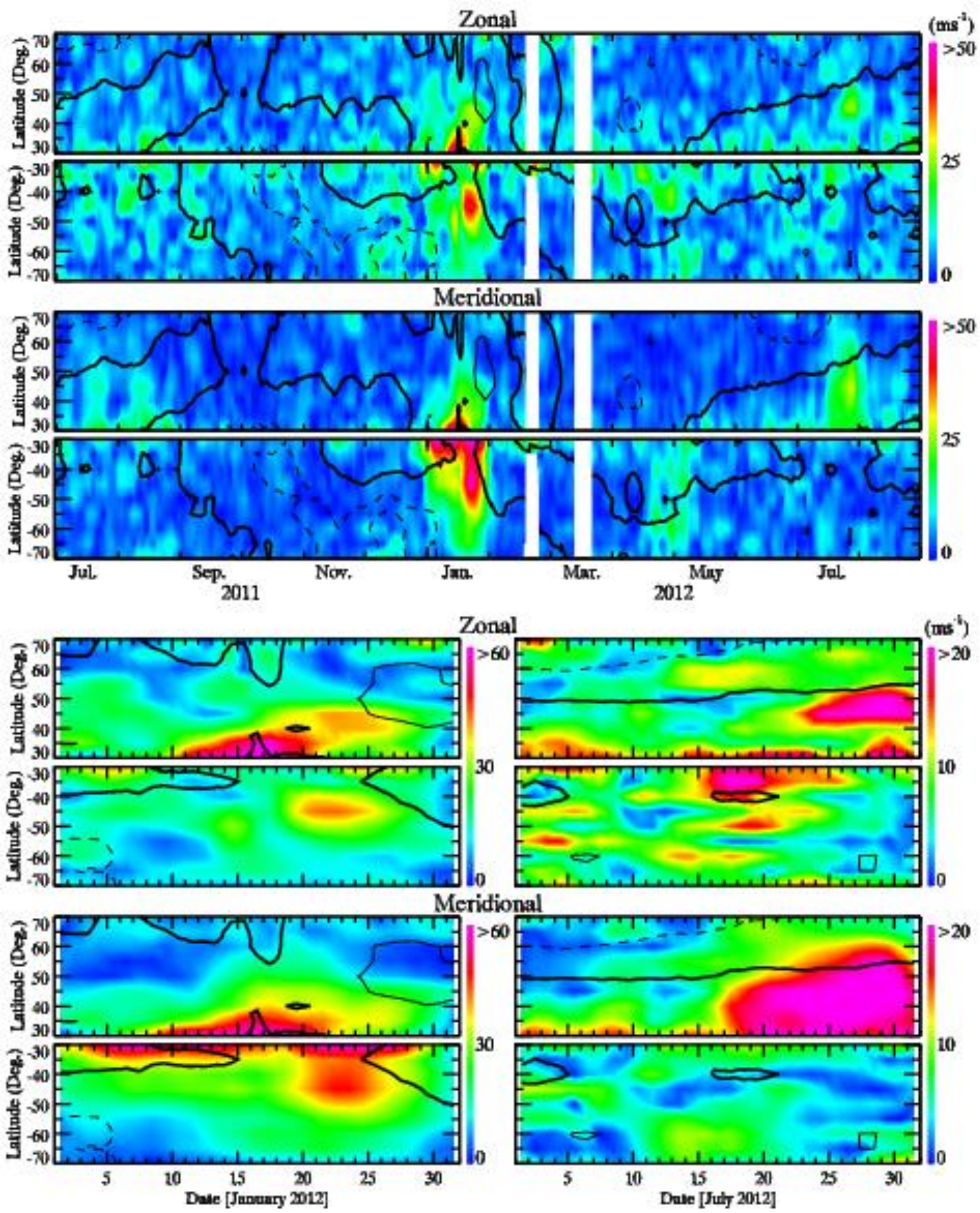

Figure 3. (Top) Q2DW amplitudes induced by MLS/balance winds at 91 km as functions of latitude from July 2011 to August 2012. (Bottom) Q2DW amplitudes of the (upper) zonal and (lower) meridional components for (left) January and (right) July 2012. Line contours are zonal mean zonal winds, defined as in Figure 1.

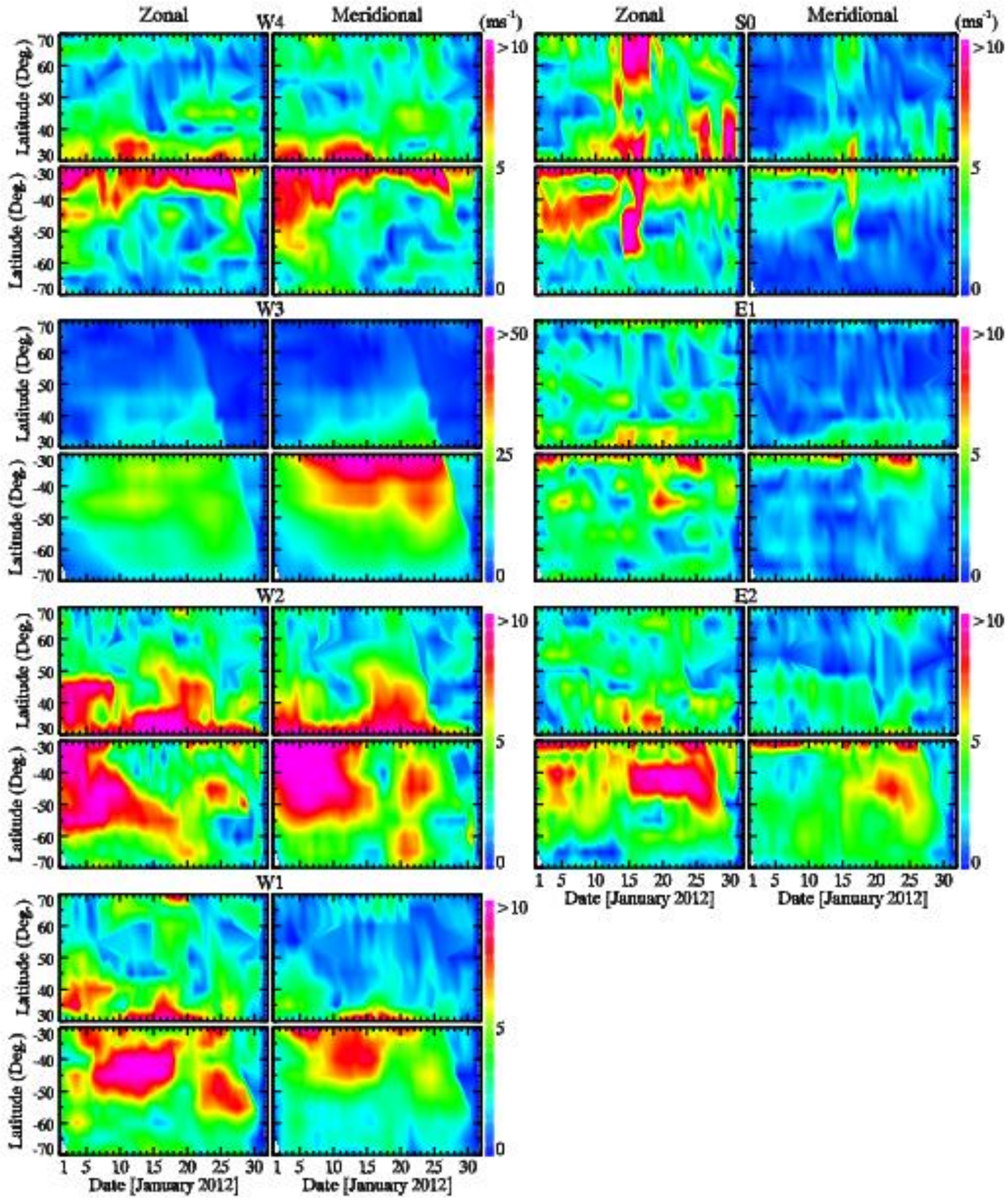

Figure 4. Q2DW zonal and meridional wind amplitudes induced by MLS/balance winds at 91 km as functions of latitude in January 2012. (Left) W4 to W1 and (right) S0 to E2 are shown from top to bottom.

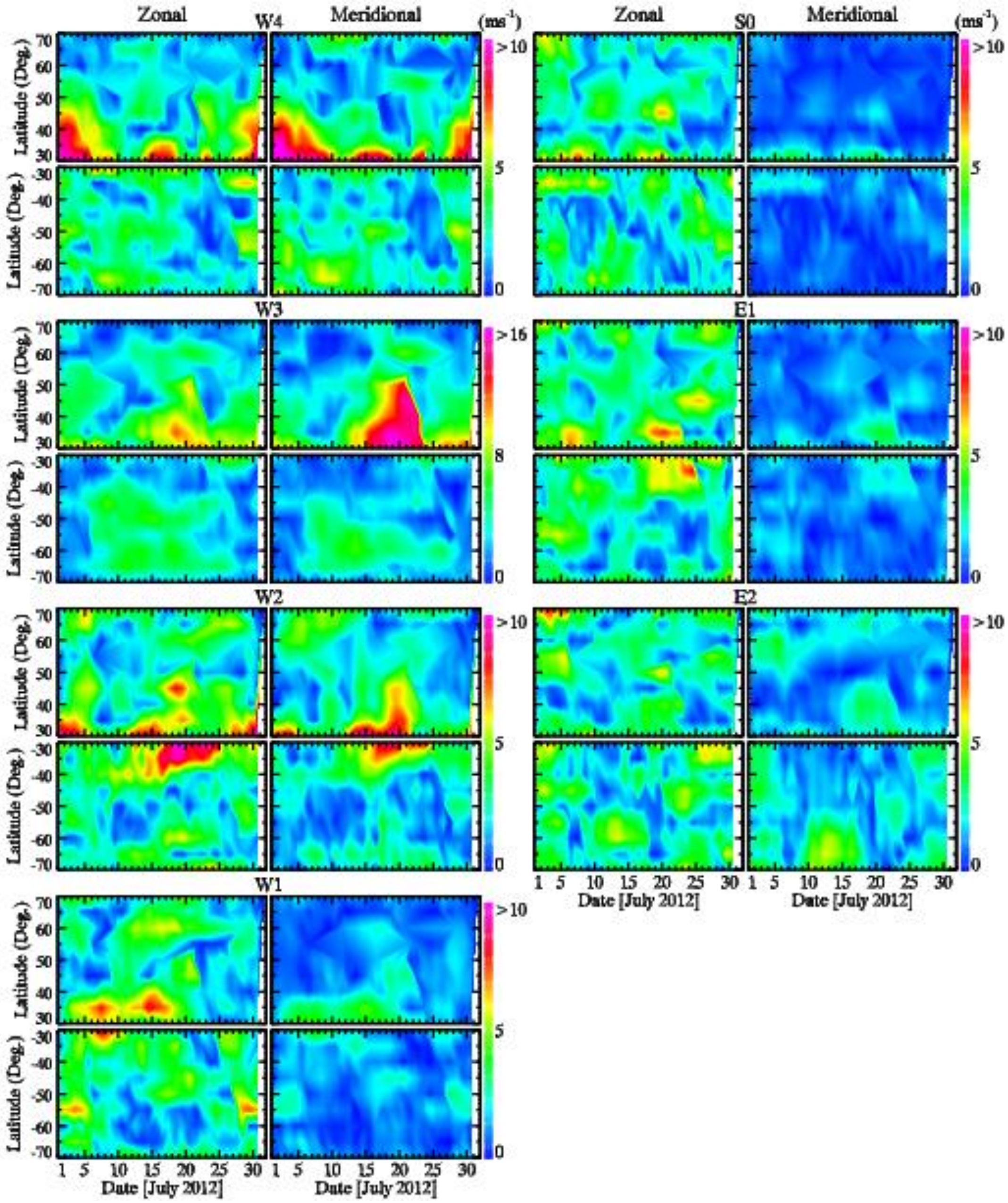

Figure 5. Same as Figure 4, but for July 2012.

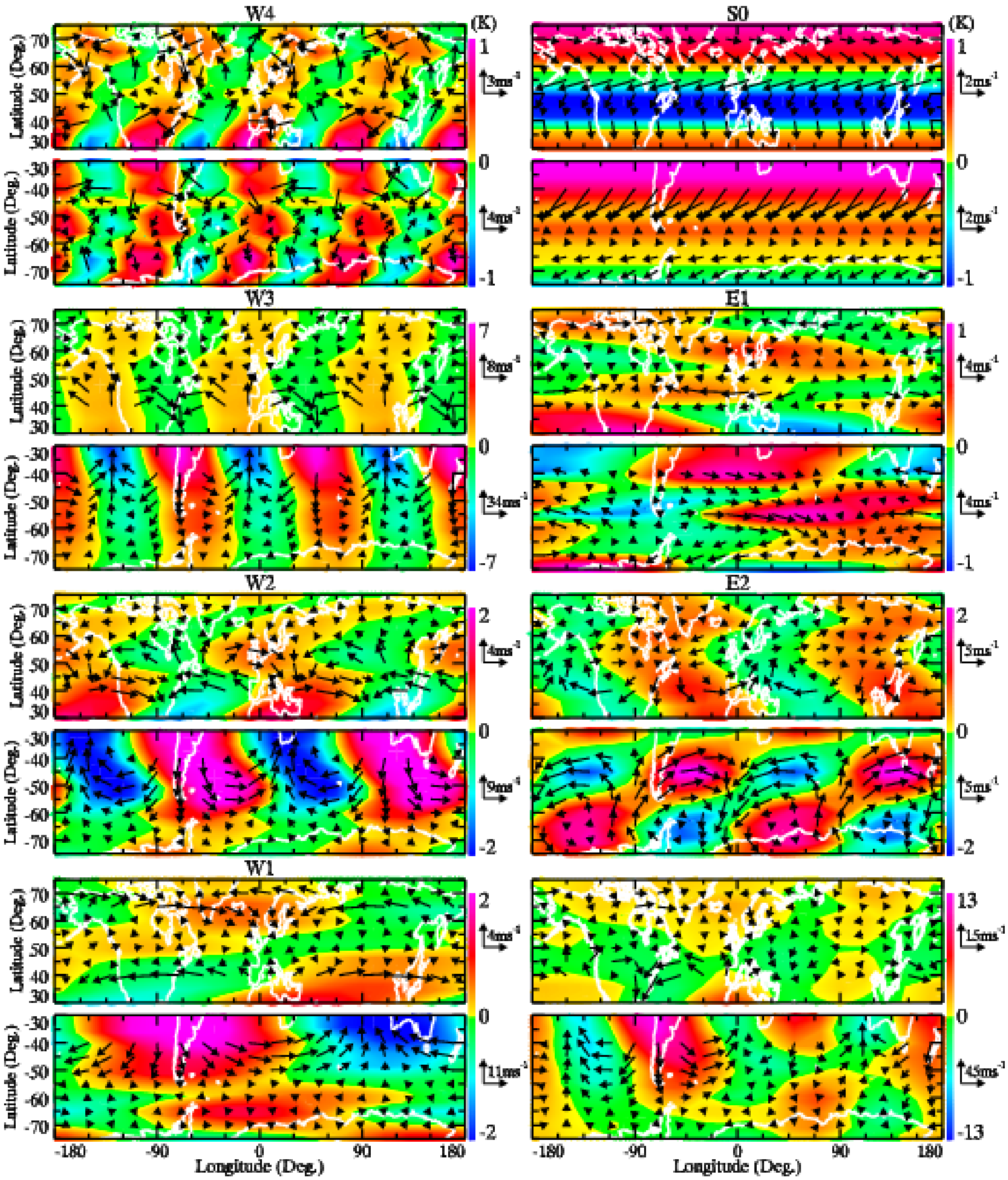

Figure 6. Longitude/latitude variations of Q2DW horizontal balance winds and MLS temperature at 91 km at 12:30 on 11 January 2012 (left) from W4 to W1 and (right) from S0 to E2, and (right bottom) sum of all modes. Note that arrow scales for winds differ between the hemispheres while color scales for temperature are same.

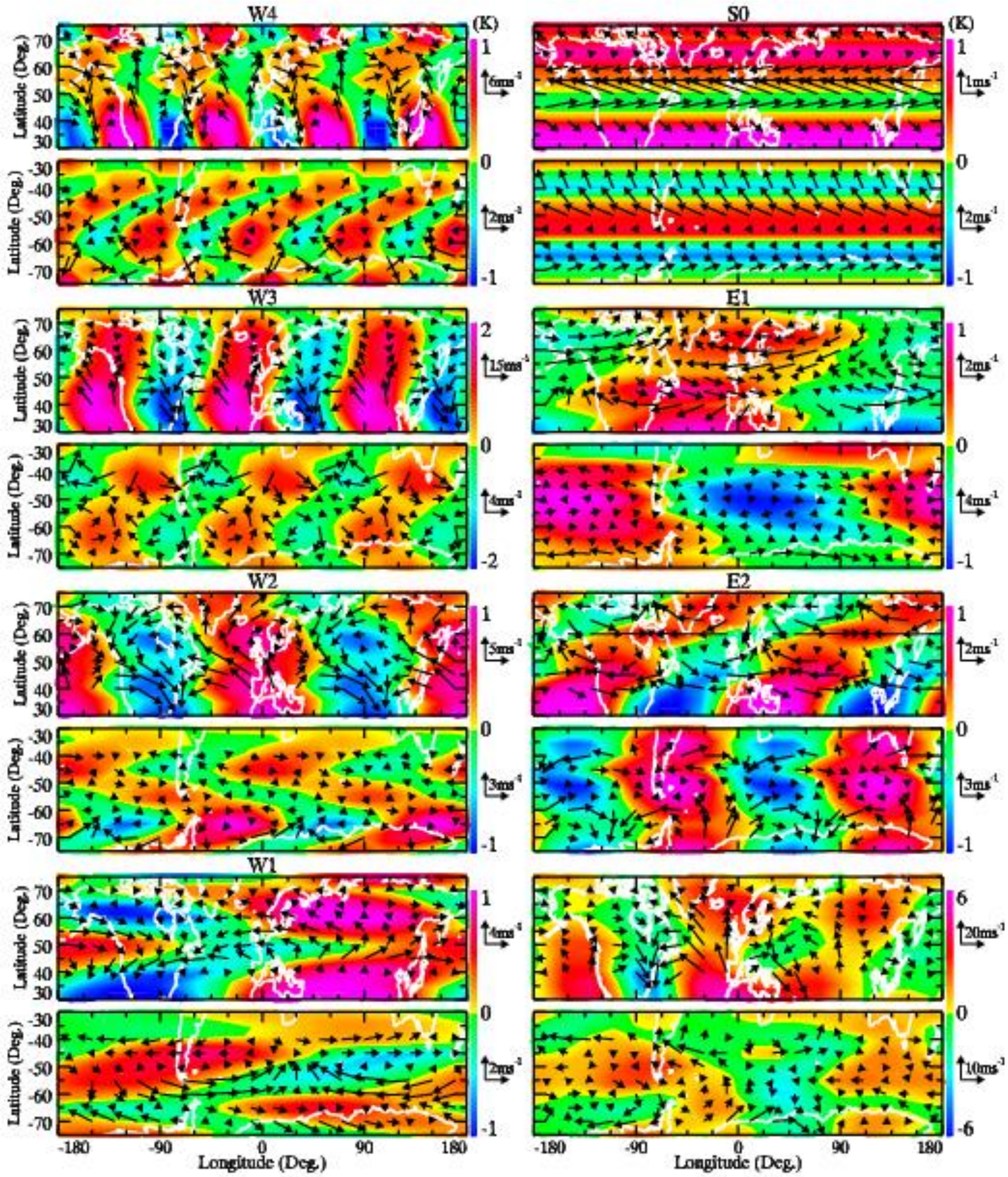

Figure 7. Same as Figure 6, but at 12:30 on 28 July 2018.

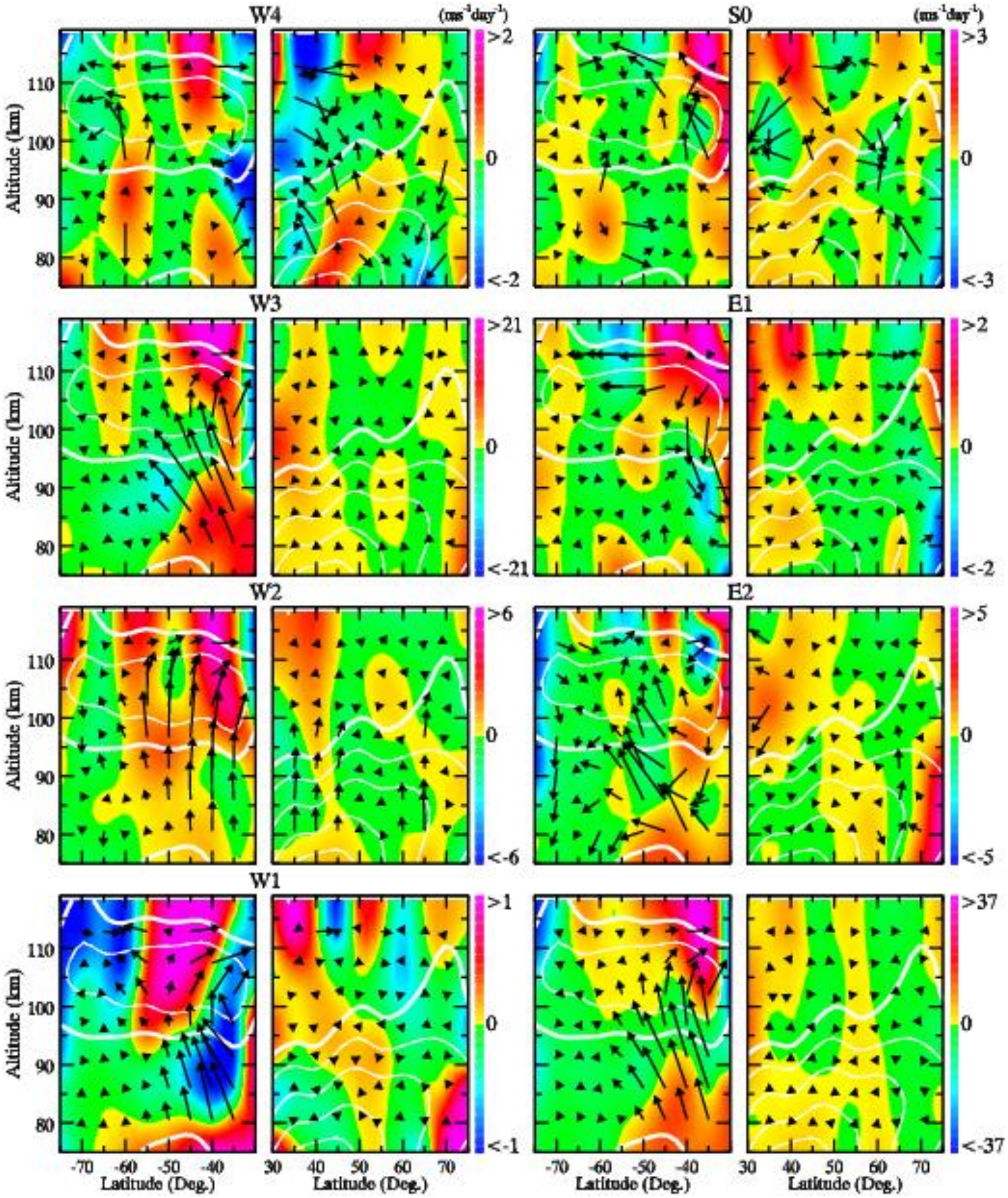

Figure 8. Latitude/altitude cross section of EP fluxes for each zonal wavenumber mode (W4 to W1 on left and S0 to E2 on right), and sum of zonal wavenumbers at right bottom on 22 January 2012. Color contours show EP flux divergence. White line contours indicate zonal mean zonal winds every 10 ms^{-1} with thick lines for 0 ms^{-1} and dashed lines for westward.

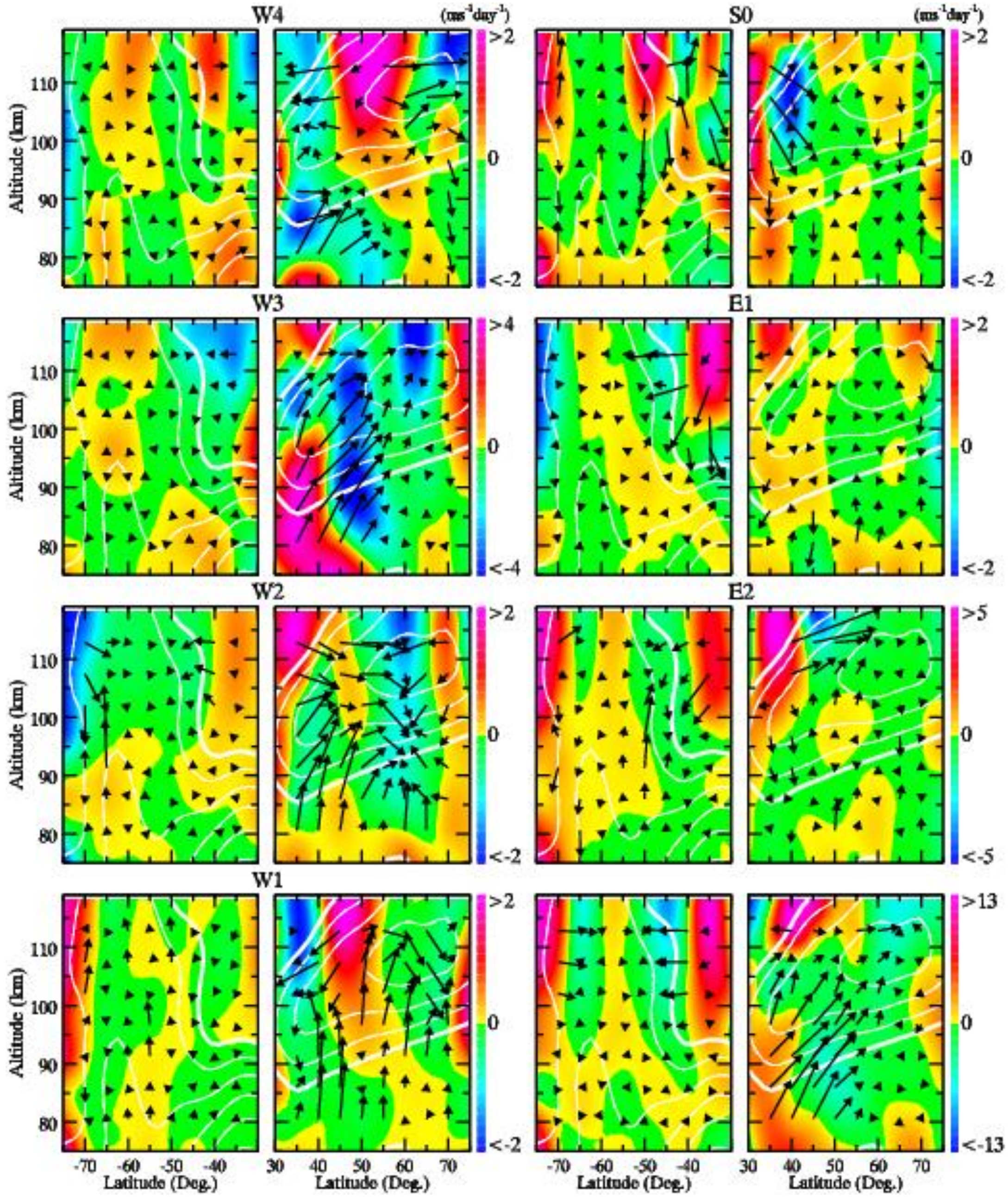

771

772 Figure 9. Same as Figure 10, but for 27 July 2012.

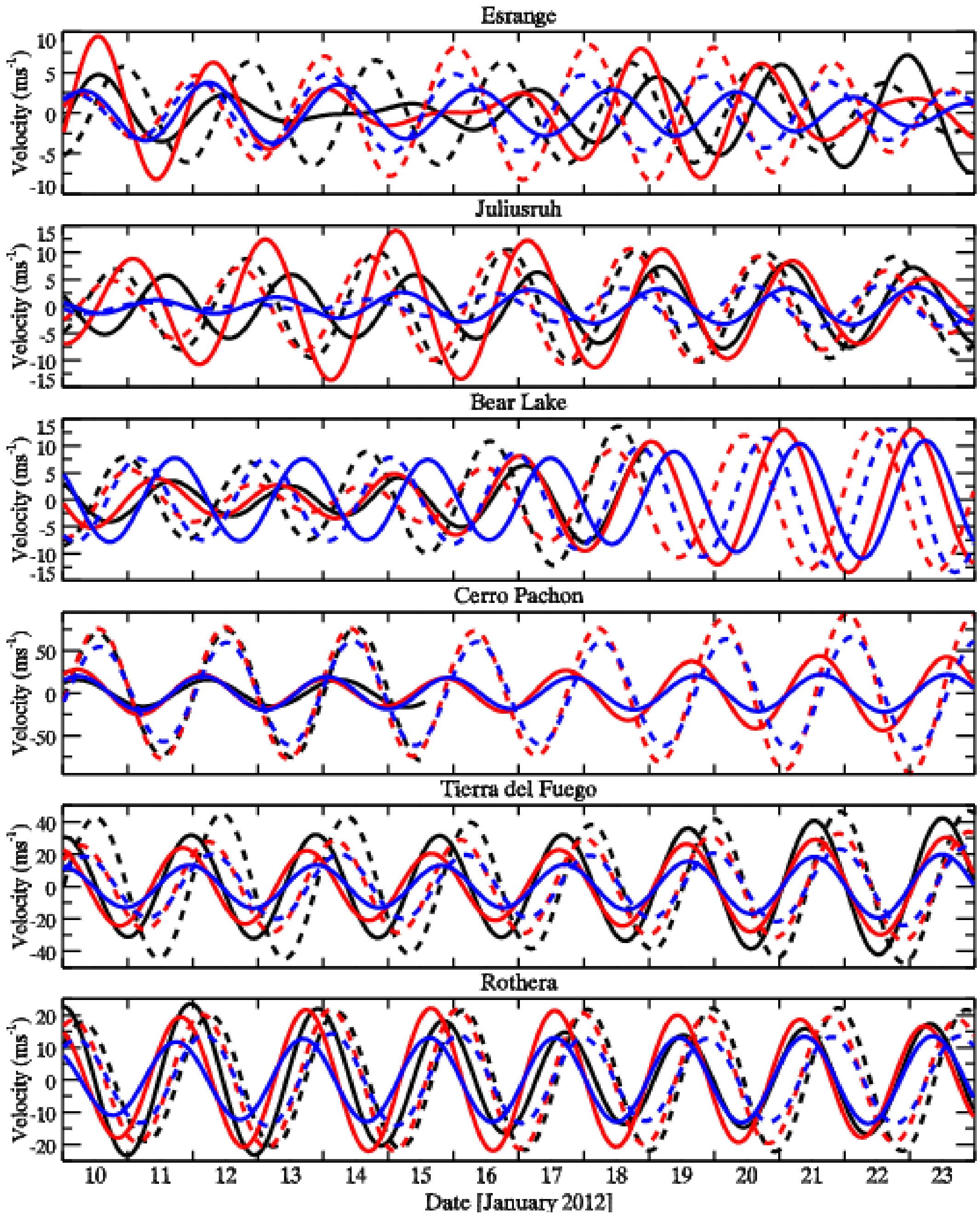

Figure 10. Time series of Q2DW in meteor radar winds at Esrange, Juliusruh, Bear Lake, Cerro Pachón, Tierra del Fuego, and Rothera at 90 km, and balance winds at closest latitudes at 91 km from 10 to 23 January 2012. Solid and dashed lines are for zonal and meridional winds, respectively. Black, red, and blue indicate meteor radar Q2DWs and balance wind Q2DWs, and W3, respectively.

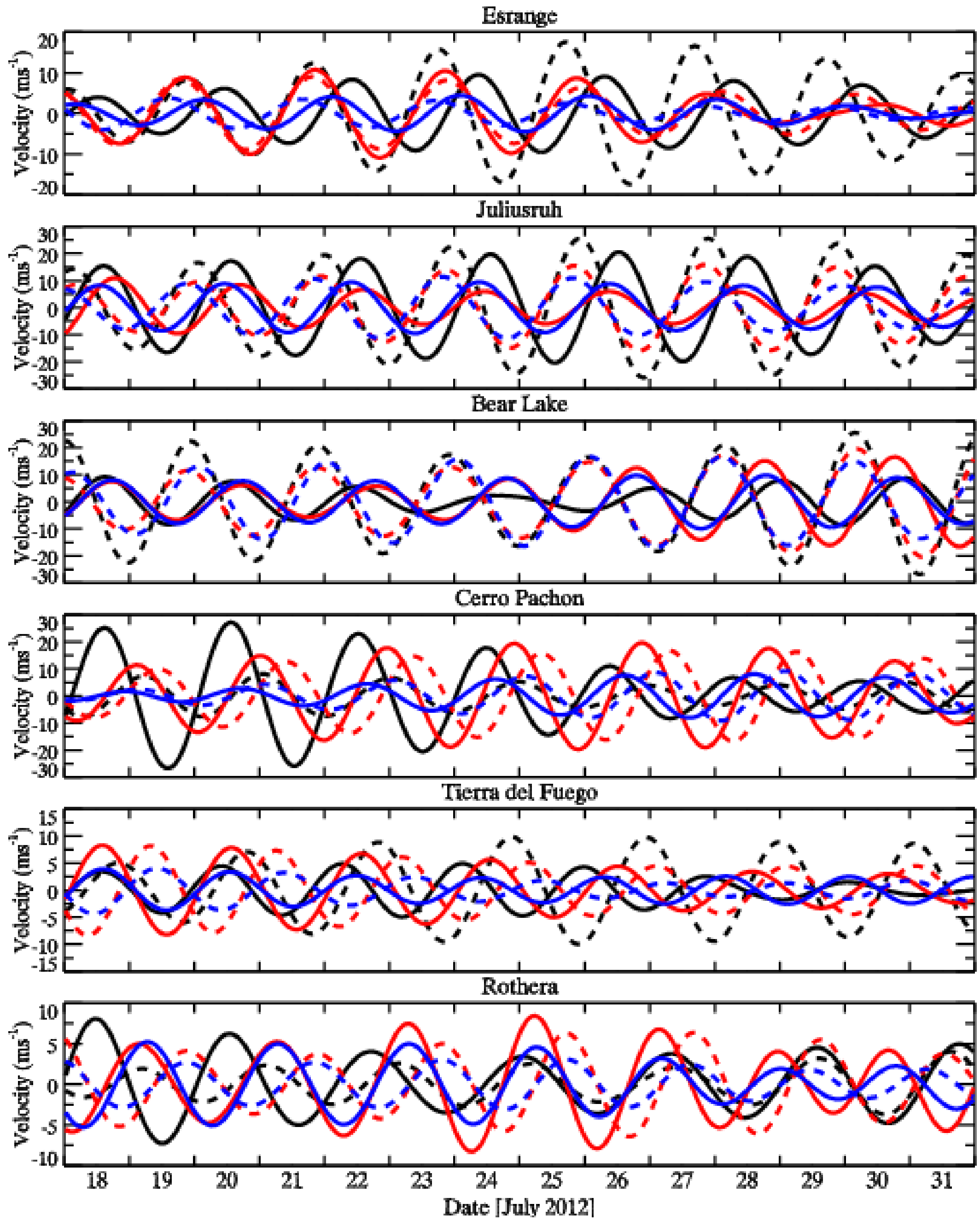

Figure 11. Same as Figure 12, but from 18 to 31 July 2012.

Figure 1.

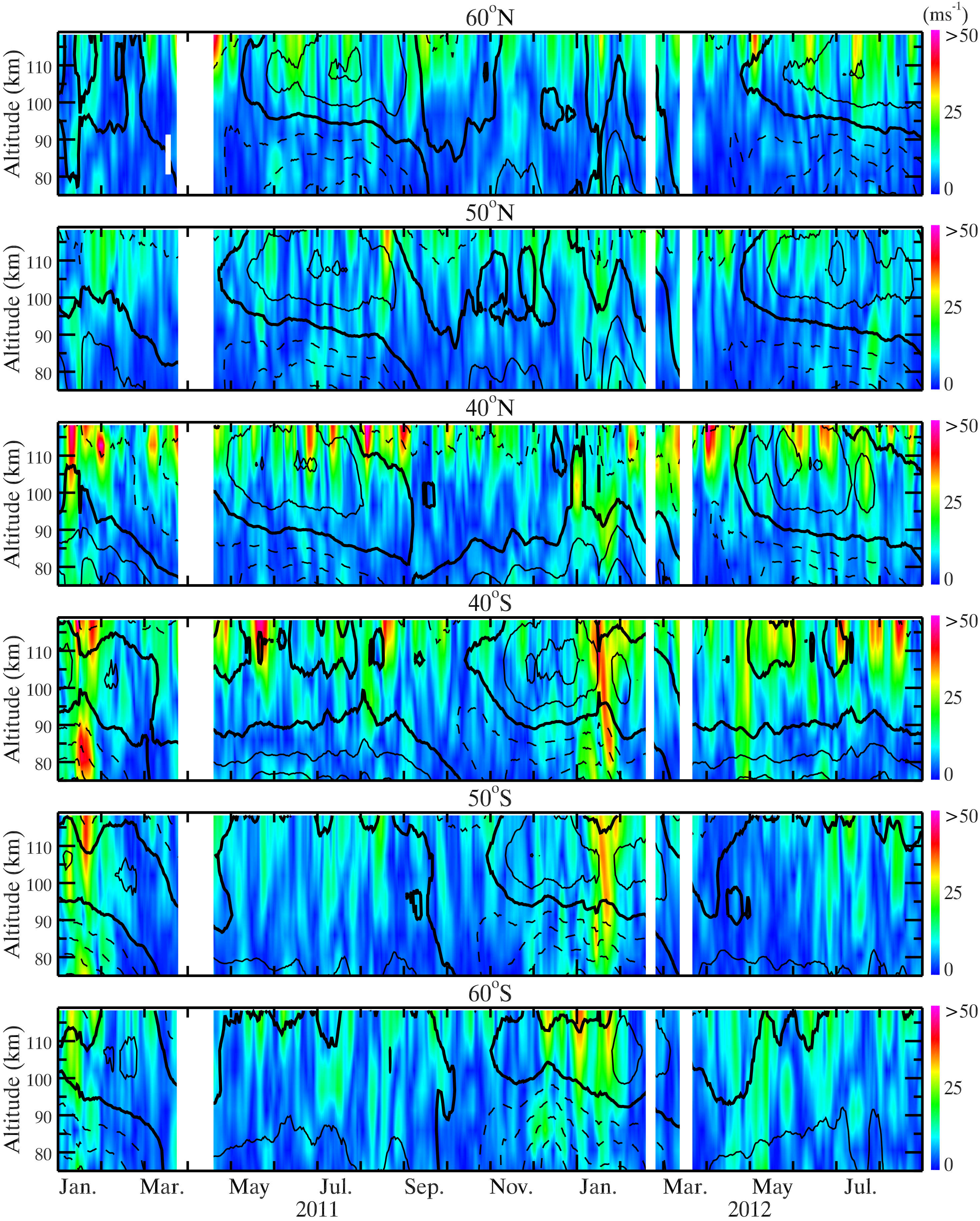

60°N
50°N
40°N
40°S
50°S
60°S
(ms⁻¹)
>50
25
0
Altitude (km)
80
90
100
110
Jan.
Mar.
May
Jul.
Sep.
Nov.
Jan.
Mar.
May
Jul.
2011
2012

Figure 2.

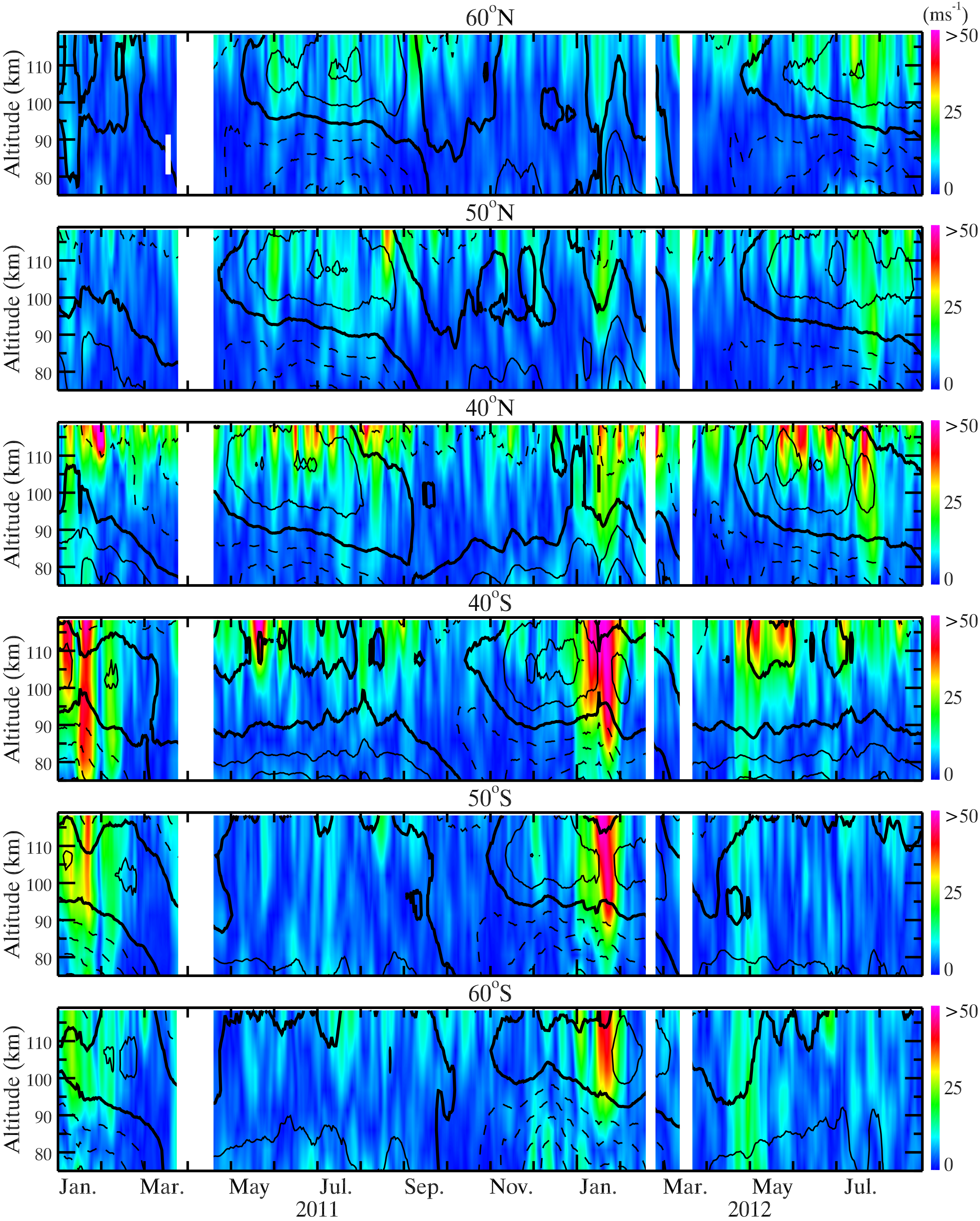

60°N
50°N
40°N
40°S
50°S
60°S
Altitude (km)
80
90
100
110
(ms⁻¹)
>50
25
0
Jan.
Mar.
May
Jul.
Sep.
Nov.
Jan.
Mar.
May
Jul.
2011
2012

Figure 3.

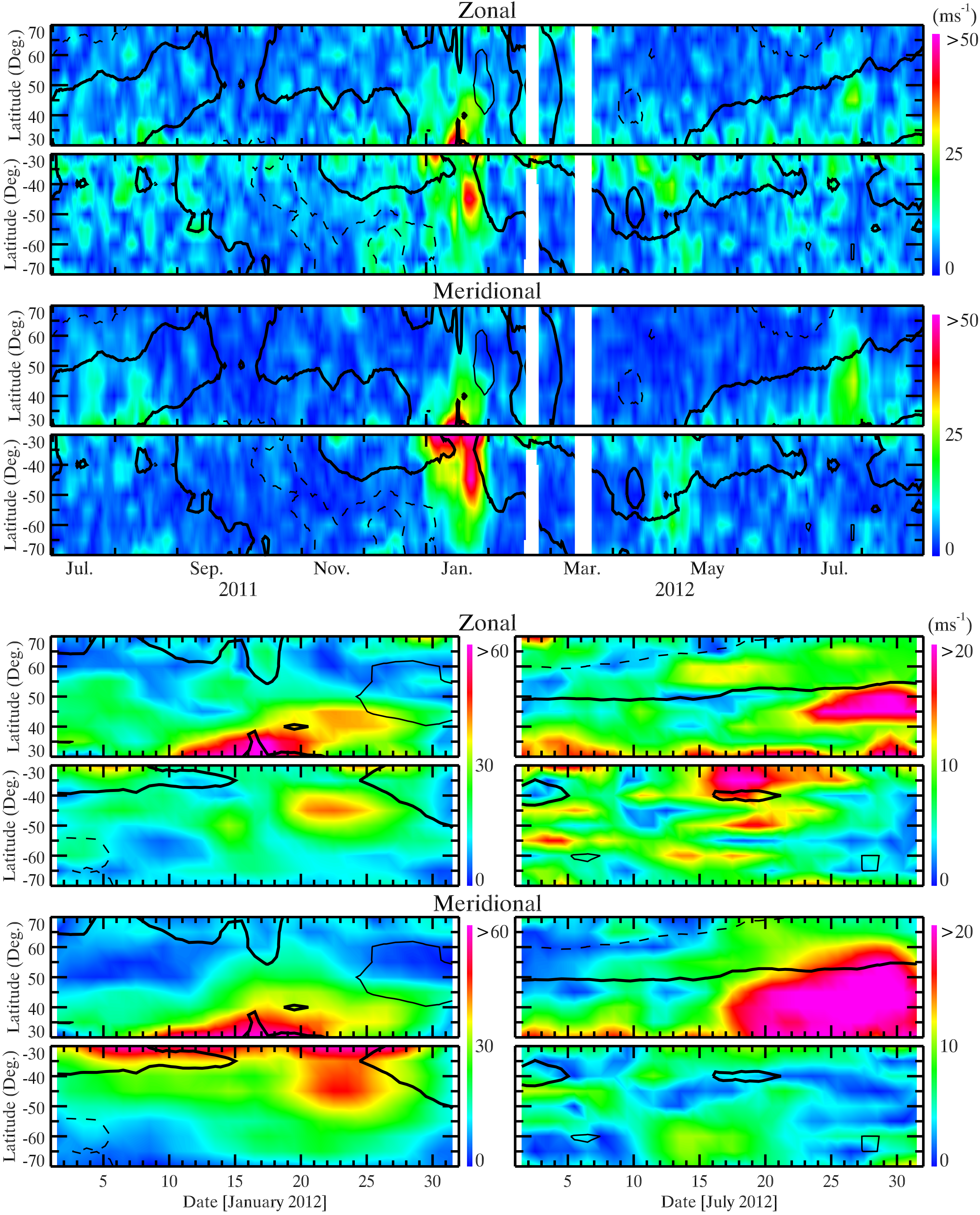

Zonal
Meridional
(ms-1)
>50
25
0
Latitude (Deg.)
70
60
50
40
30
-30
-40
-50
-60
-70
Jul.
Sep.
Nov.
Jan.
Mar.
May
Jul.
2011
2012
Zonal
Meridional
(ms-1)
>60
30
0
>20
10
0
5
10
15
20
25
30
Date [January 2012]
Date [July 2012]

Figure 4.

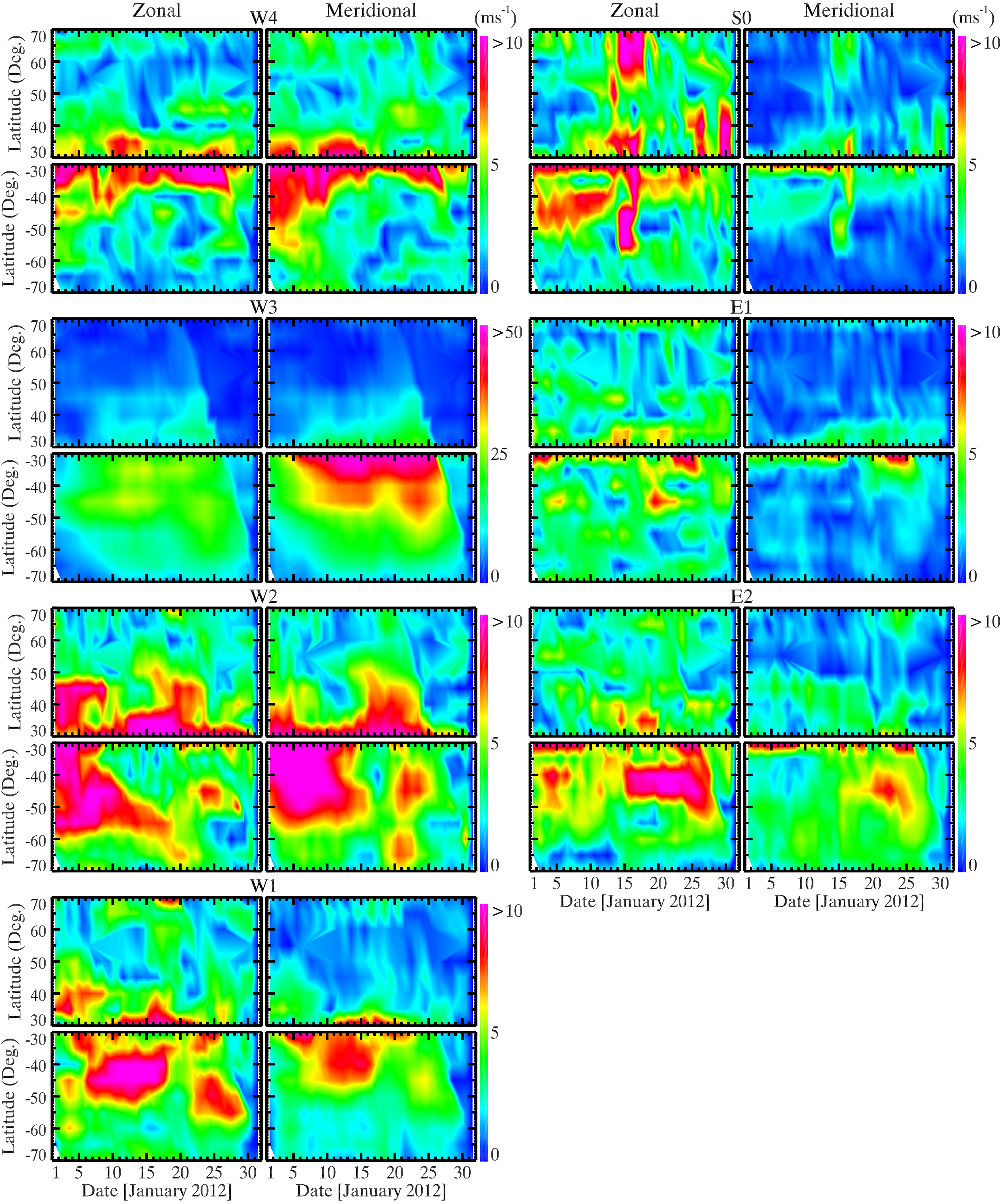
Zonal
Meridional
Zonal
Meridional
(ms-1)
W4
S0
W3
E1
W2
E2
W1
Latitude (Deg.)
>10
>50
25
5
0
Date [January 2012]

Figure 5.

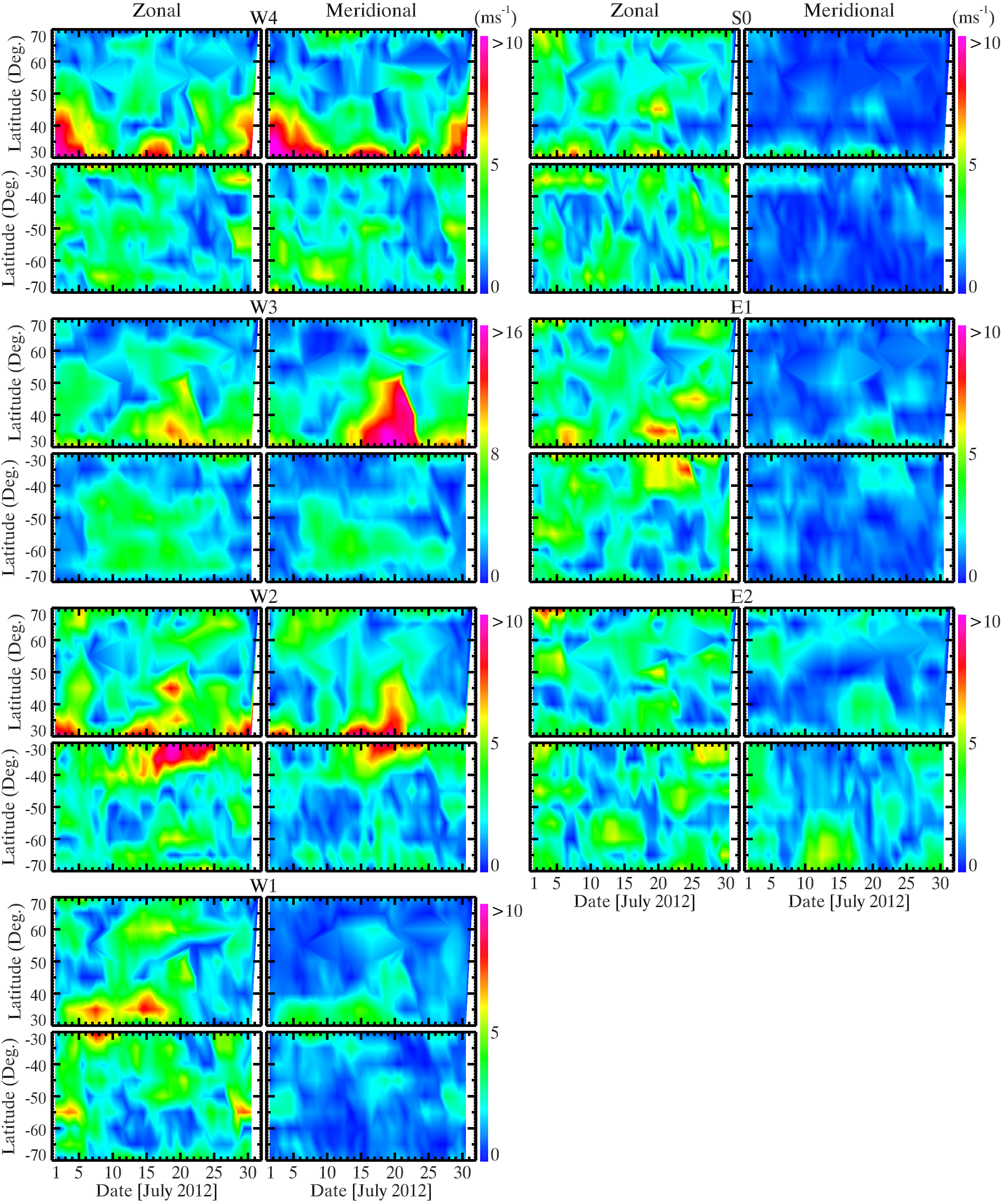

Zonal
Meridional
(ms-1)
W4
S0
W3
E1
W2
E2
W1
>10
>16
5
8
0
Latitude (Deg.)
70
60
50
40
30
-30
-40
-50
-60
-70
1
5
10
15
20
25
30
Date [July 2012]

Figure 6.

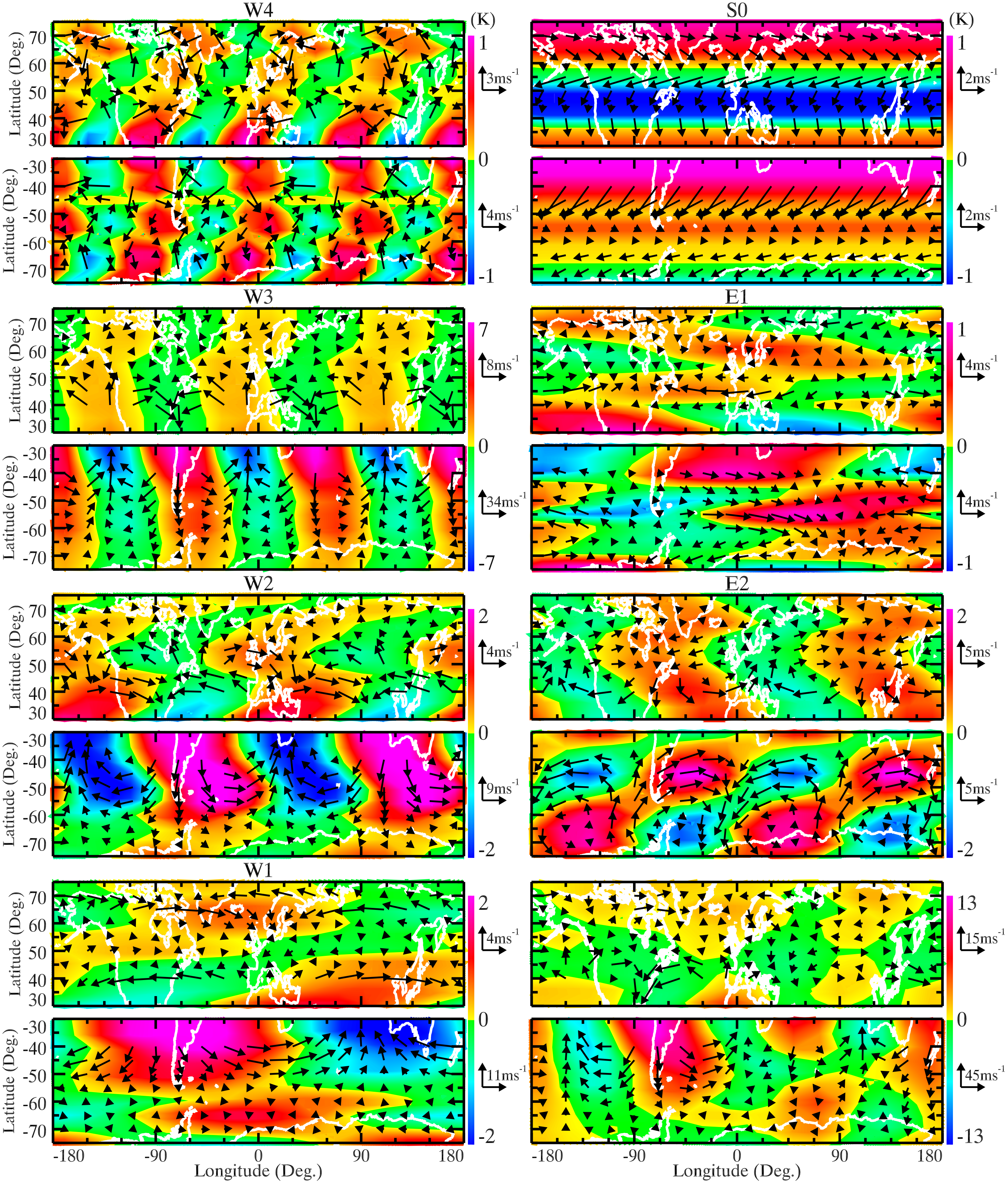

W4
S0
W3
E1
W2
E2
W1
(K)
1
0
-1
7
-7
2
-2
13
-13
3ms-1
4ms-1
2ms-1
8ms-1
34ms-1
9ms-1
5ms-1
11ms-1
15ms-1
45ms-1
Latitude (Deg.)
Longitude (Deg.)
-180
-90
0
90
180
70
60
50
40
30
-30
-40
-50
-60
-70

Figure 7.

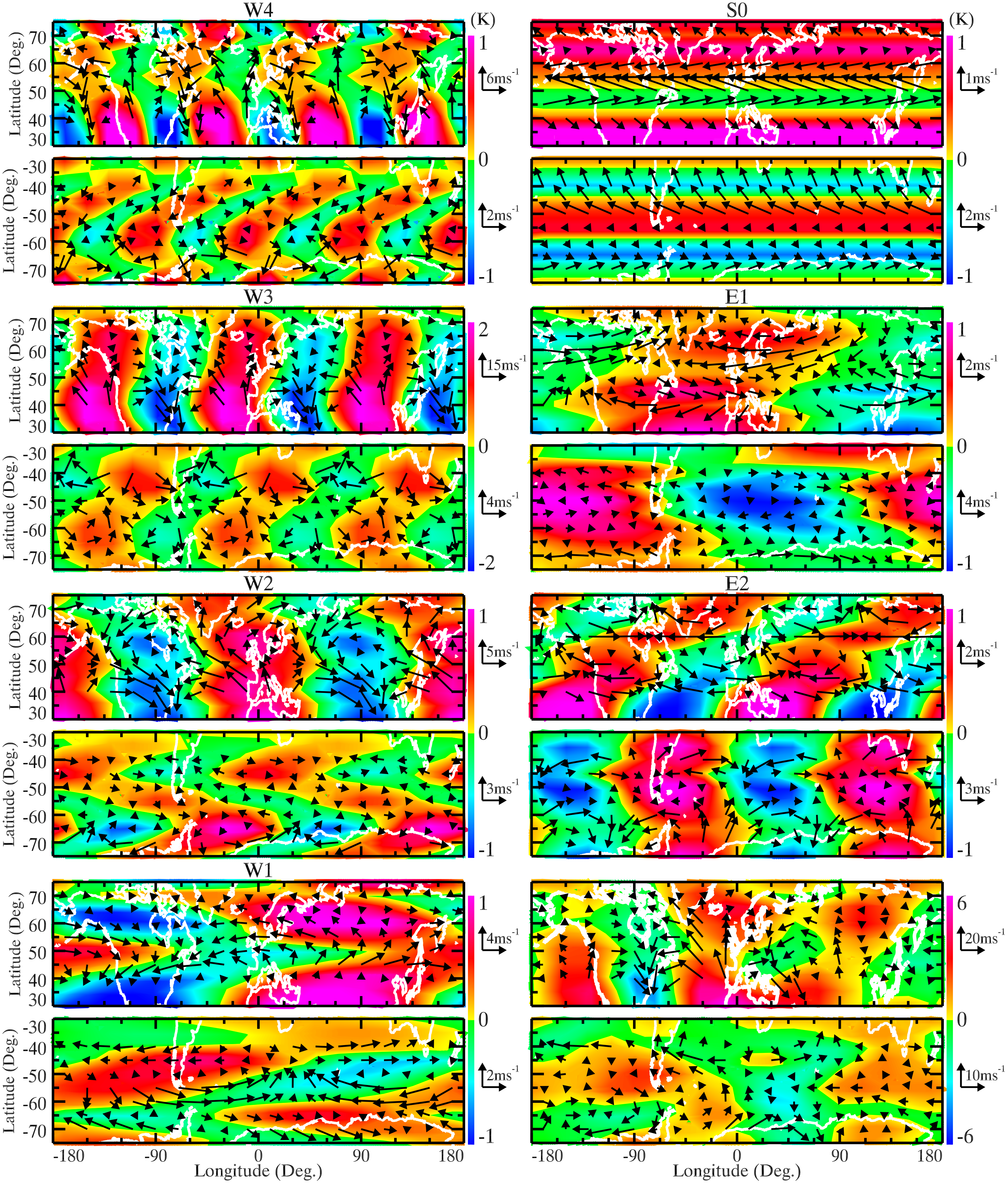
W4
S0
W3
E1
W2
E2
W1
(K)
Latitude (Deg.)
Longitude (Deg.)
6ms-1
2ms-1
1ms-1
15ms-1
4ms-1
5ms-1
3ms-1
20ms-1
10ms-1
-180
-90
0
90
180

Figure 8.

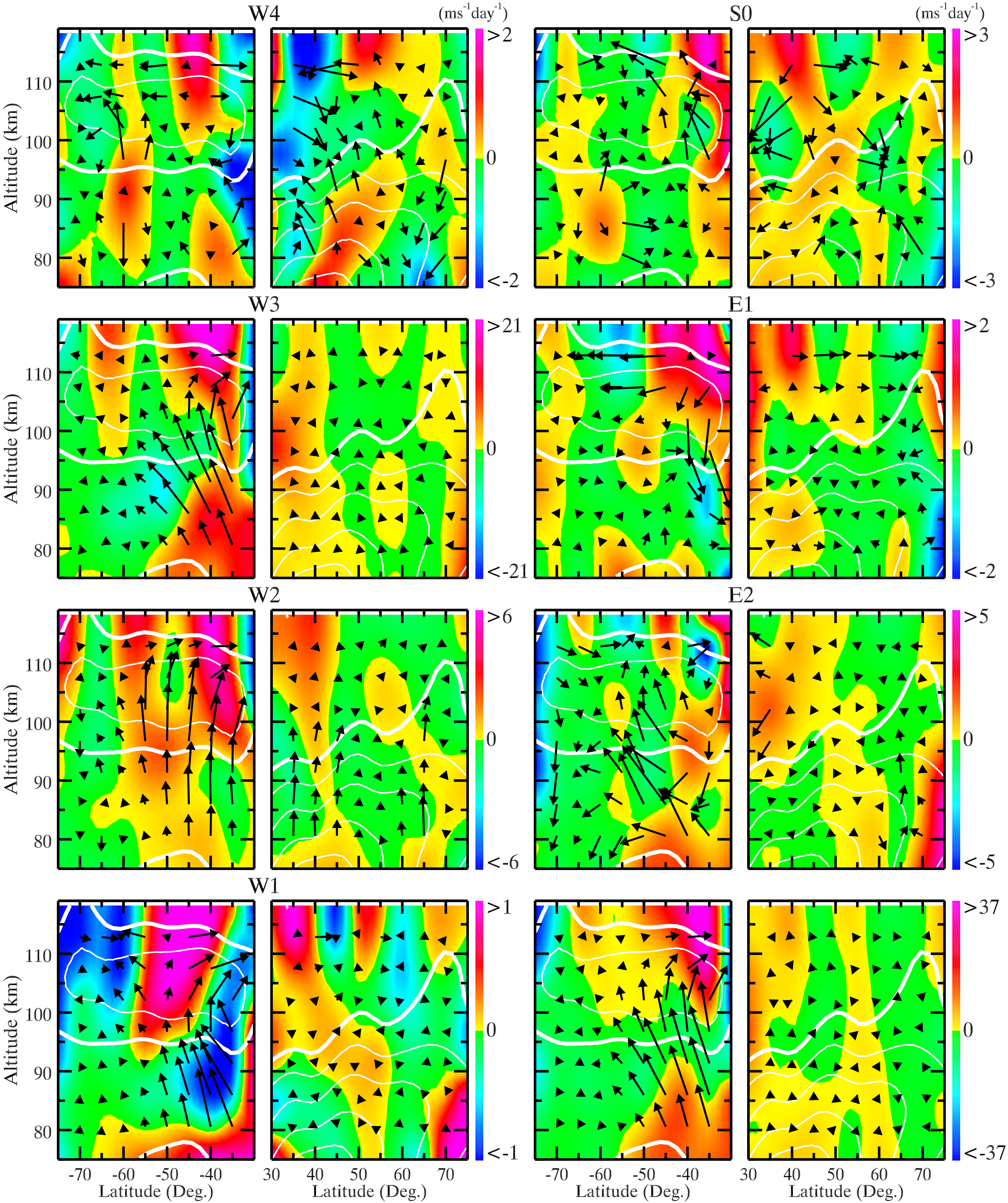
W4
S0
W3
E1
W2
E2
W1
(ms^{-1}day^{-1})
>2
0
<-2
>3
<-3
>21
<-21
>2
<-2
>6
<-6
>5
<-5
>1
<-1
>37
<-37
Altitude (km)
Latitude (Deg.)

Figure 9.

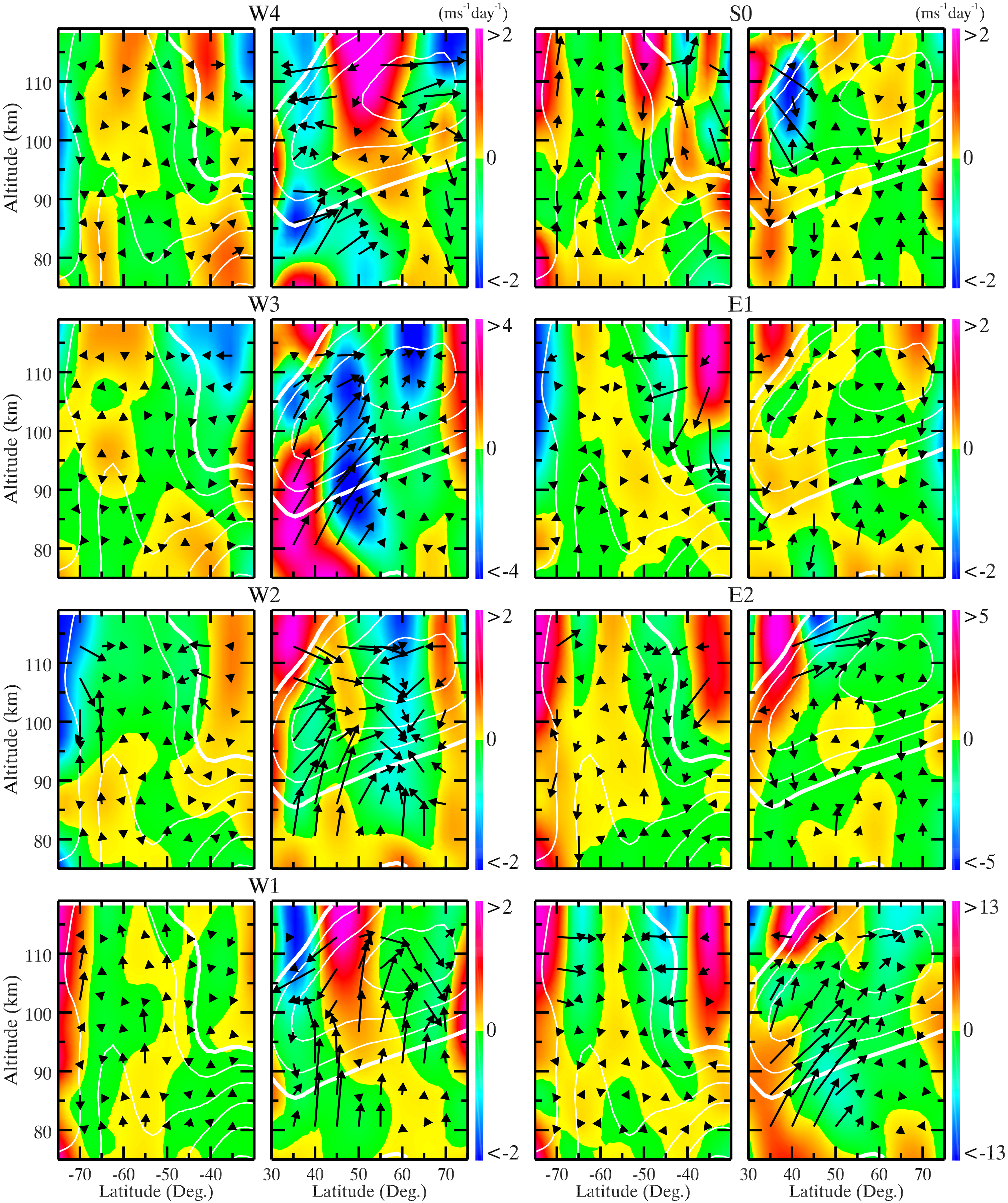

W4
S0
W3
E1
W2
E2
W1
(ms^{-1}day^{-1})
>2
0
<-2
>4
<-4
>5
<-5
>13
<-13
Altitude (km)
Latitude (Deg.)

Figure 10.

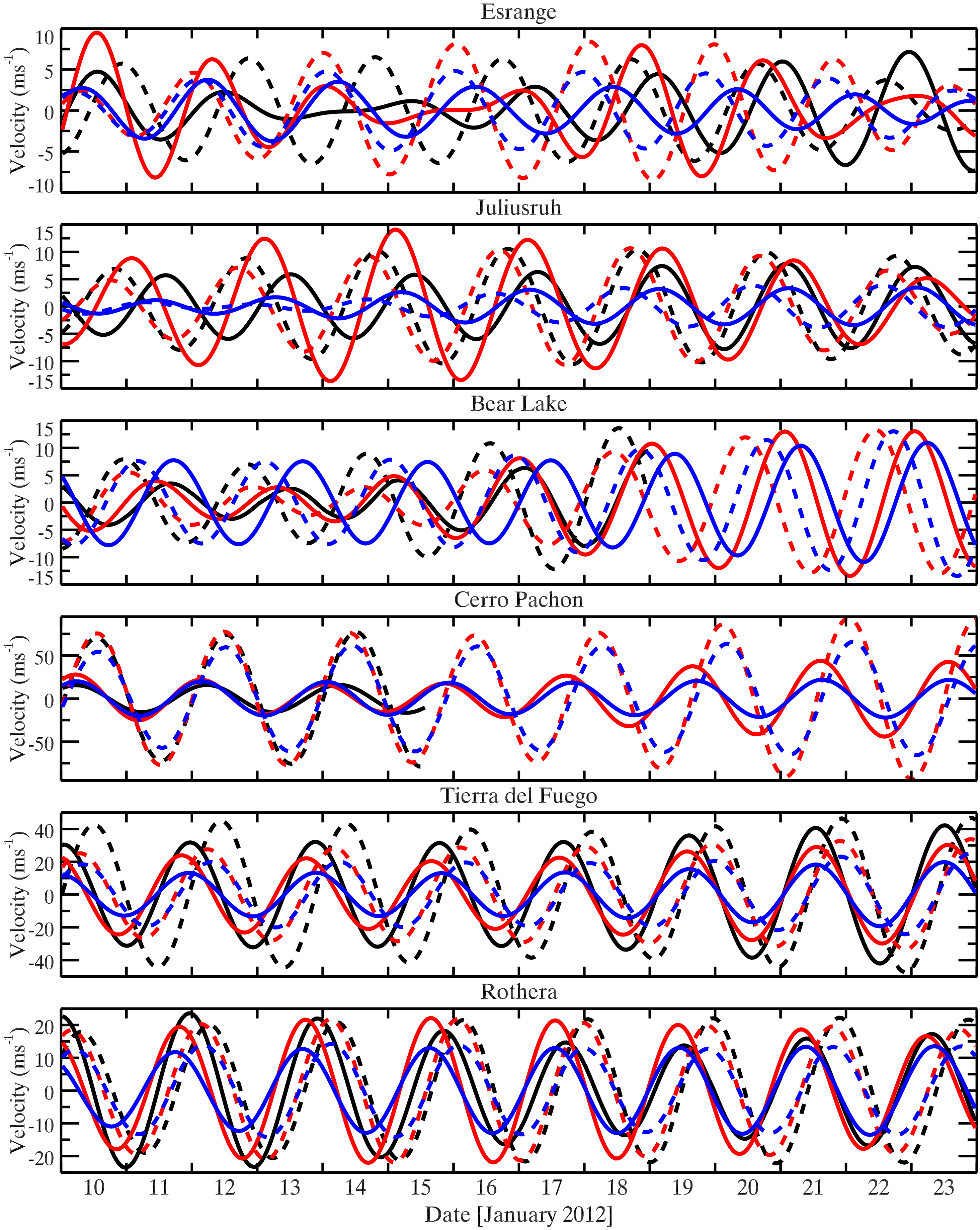

Esrange
Juliusruh
Bear Lake
Cerro Pachon
Tierra del Fuego
Rothera
Velocity (ms^{-1})
Date [January 2012]
10
11
12
13
14
15
16
17
18
19
20
21
22
23

Figure 11.

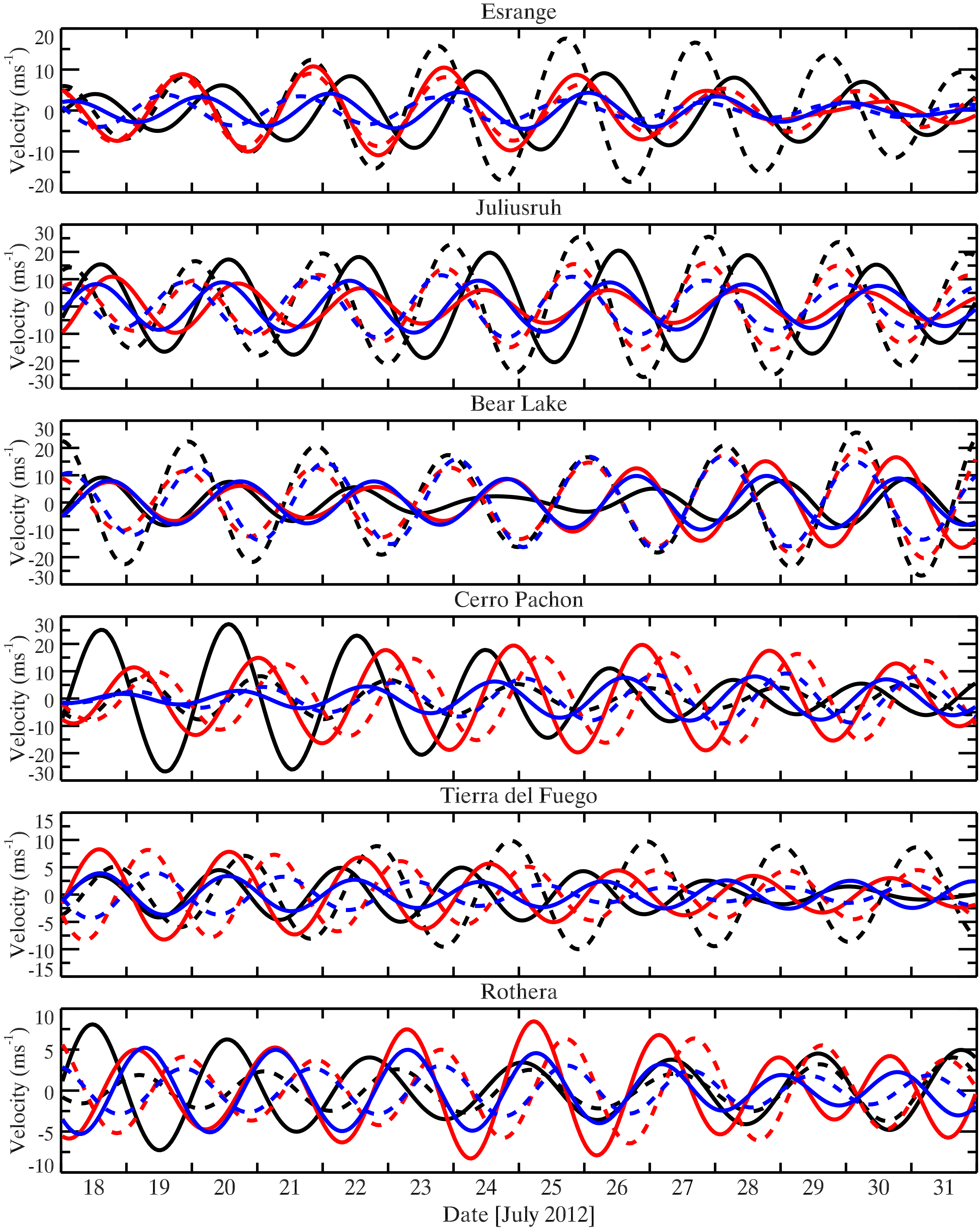

Esrange
Juliusruh
Bear Lake
Cerro Pachon
Tierra del Fuego
Rothera
Velocity (ms⁻¹)
Date [July 2012]
18
19
20
21
22
23
24
25
26
27
28
29
30
31